

# Study of vibrational spectra of polycyclic aromatic hydrocarbons with phenyl side group

Anju Maurya, Rashmi Singh and Shantanu Rastogi\*

Department of Physics, D.D.U. Gorakhpur University, Gorakhpur, India - 273009

\* e-mail: shantanu\_r@hotmail.com

## Abstract

Computational study of polycyclic aromatic hydrocarbons (PAHs) with phenyl side group substituted at different positions is reported. The infrared spectral variations due to the position of phenyl substitution, ionization state and the size of the molecules are discussed and possible contribution of phenyl-PAHs to the mid-infrared emission features from astrophysical objects is analyzed. Structurally phenyl group substitution at 2<sup>nd</sup> position gives more stable species compared to substitution at other positions. Phenyl-PAHs exhibit new aromatic bands near 695 and 741 cm<sup>-1</sup> (14.4 and 13.5  $\mu$ m), due to contribution from quintet C-H wag, that compare well with minor features at 14.2 and 13.5  $\mu$ m observed in several astrophysical objects. Just as in plain PAHs, the C-C stretch vibrational modes ( $\sim$ 1600 cm<sup>-1</sup>) have negligible intensity in neutrals, but the cations of all phenyl-PAHs exhibit significantly strong phenyl group C-C stretch peak close to class B type 6.2  $\mu$ m astrophysical band. In 2-phenylpyrene, it is the neutral molecule that exhibits this strong feature in the 6.2  $\mu$ m range along with other features that match with sub-features at 6.66 and 6.9  $\mu$ m, observed in astronomical spectra of some late type objects. The substitution of phenyl side group at solo position shifts the C-C stretch mode of parent PAH close to the region of 6.2  $\mu$ m astrophysical band. The results indicate possibility of phenyl-PAHs in space and the bottom-up formation of medium sized compact PAHs with phenyl side group in carbon rich cool circumstellar shells. Phenyl-PAHs need to be considered in modelling mid-infrared emission spectra of various astrophysical objects.

## keywords:

PAH; Aromatic Infrared Bands; Interstellar molecules; DFT calculations; Astrochemistry

## 1 Introduction

Polycyclic Aromatic Hydrocarbons (PAHs) are considered to be ubiquitous and among abundant species in the interstellar medium (ISM) [1, 2, 3, 4]. This is due to the presence of mid-infrared emission bands, which are most prominent at 3.3, 6.2, 7.7, 8.6, 11.2 and 12.7  $\mu$ m (3030, 1610, 1300, 1160, 890 and 790 cm<sup>-1</sup>), in a

wide variety of astrophysical sources [5, 6, 7, 8, 9, 10]. These features correspond to the vibrational transitions in aromatic molecules and are, therefore, referred to as aromatic infrared bands (AIBs). PAHs in the ISM form around carbon-rich AGB stars and evolve through harsh astrophysical environments leaving only the most stable species in the ISM [3, 11]. The mechanism of infrared emission involves absorption of ultraviolet photons from background sources (viz. hot central remnant in evolved stars or hot young O/B associations in star forming regions) and redistribution of this energy into the vibrational modes that fluoresces in the infrared [12, 13]. The resulting AIBs carry signatures of the collection of PAHs present in the environment.

The variation in the profile of AIB features correlates with type of astrophysical object, indicating different PAH types and populations in different regions [14, 15, 16, 17]. The modelled emission spectra using quantum chemical data for a large set of PAHs show good match for the 7.0 - 9.0  $\mu\text{m}$  AIB range from different sources [16, 17, 18, 19]. Despite the general similarity of AIBs to PAH vibrational spectrum and some feature correlations, the simultaneous matching of all AIBs has not been possible. In particular the 6.2  $\mu\text{m}$  feature and few features between 10 - 15  $\mu\text{m}$  remain unmatched. When plain PAHs are considered the aromatic C-C stretching modes fall short by 30 - 40  $\text{cm}^{-1}$  of the 6.2  $\mu\text{m}$  AIB [16]. To address these problems studies incorporating derivatives such as substituted PAHs, hydrogenated PAHs, dehydrogenated PAHs, protonated PAHs, PAHs with nitrogen heterocycles, vinyl-PAHs etc. [20, 21, 22, 23, 24, 25, 26, 27, 28] have been attempted with none or partial improvement.

The emissions between 10 - 15  $\mu\text{m}$  reveal weak features [18, 19] that too remain unexplained by the C-H out-of-plane modes of peripheral hydrogen atoms in plain PAHs. The IR activity of C-H out-of-plane bend modes is governed by the number of dangling H atoms in an aromatic ring [29]. The bands in 13.0 - 13.7  $\mu\text{m}$  region indicate quartet (four adjacent Hydrogens in a ring) while quintet (five adjacent Hydrogens in a ring) have additional features in 14.0 - 14.5  $\mu\text{m}$  range [29, 30, 31]. Quintet modes are possible only in phenyl group. The phenyl radical has infrared spectrum similar to benzene and other neutral PAHs, with a very weak C-C stretch mode at 1624  $\text{cm}^{-1}$  [32]. But, the same phenyl as a side group, on aliphatic compounds and even in complex systems [33, 34], has a medium intense feature close to the 6.2  $\mu\text{m}$  AIB.

The formation of aromatics in space is interpreted via combustion chemistry [35], wherein phenyl radical is an important intermediate and may play a major role in chemistry of the ISM [36, 37]. Modelling protoplanetary nebula conditions, of dense-warm gas irradiated by an strong UV field, has shown to produce benzene [38]. The presence of CN could further lead to the formation of benzonitrile [38], which is reported to have been detected in Taurus Molecular Cloud [39]. Thus,

the presence of phenyl group in the ISM is strongly indicated. Pyrolysis of simple aromatics could form polyphenyls [40, 41, 42]. Phenyl-PAHs are also obtained in laboratory study of shock against benzene [43]. Such shock conditions are possible in the expanding envelopes of protoplanetary nebulae, suggesting a finite possibility for PAHs acquiring phenyl side group in these environments.

Considering these aspects of phenyl substitution, the vibrational spectra of biphenyl, phenylnaphthalenes, phenylanthracenes, phenylpyrenes, phenylcoronene and phenylvalene are computed. Analysis of spectral feature variations is performed for phenyl group attached at different positions on the plain PAHs. Both neutral and cation state of the molecules are considered. The possible correlations of modes close to the astrophysical AIBs are identified and discussed in the present work.

## 2 Computation and Results

The density functional theory (DFT) calculations have proved propitious in evaluating infrared spectra of PAHs [44, 45, 46, 47, 48, 49, 50] and in using them to model AIBs from different sources [16, 17, 51]. For the study of phenyl-PAHs the DFT-B3LYP method in combination with the 6-31G(d) basis set is used to obtain optimized molecular structure and infrared vibrational frequencies. The GAMESS ab initio program [52] is used for the calculations. Study of ten phenyl-PAH molecules shown in Figure 1 is performed, which include biphenyl, 1-phenylnaphthalene, 2-phenylnaphthalene, 2-phenylanthracene, 9-phenylanthracene, 1-phenylpyrene, 2-phenylpyrene, 4-phenylpyrene, 1-phenylcoronene and 14-phenylvalene. As molecules in the ISM are mostly ionized, study is performed for both neutrals and cations.

In all the molecules, the phenyl moiety is out-of-plane with respect to the parent PAH. The torsion angle for different position of phenyl substitution is in general different due to different steric hindrances. The molecular energy is computed for different out-of-plane angles of the phenyl moiety to study the behaviour near optimized minima. In biphenyl and for 2<sup>nd</sup> position substituted phenyl-PAHs, there is a sharp minima at torsion angle  $\sim 40^\circ$  (Figure 2a). While in 1 and 4 position substituted phenyl-PAHs, the optimized phenyl torsion angle is  $\sim 55^\circ$  out-of-plane of the parent PAH (Figure 2b), but the minima are not sharp and there is very little increment in energy upon increasing the torsion angle beyond the minima. The environment of the phenyl group is similar in biphenyl and 2- substituted phenyl PAHs, with symmetric placement of two adjacent hydrogen atoms. Whereas, in phenyl-PAHs substituted at 1 and 4 position there is asymmetric hydrogen placement i.e., there is only one hydrogen on the same ring as the phenyl group (Figure 1). In solo position substituted phenyl-PAHs (9-phenylanthracene and 14-phenylvalene), where there is no hydrogen on the ring with the phenyl group,

the steric interaction is negligible and the torsion angle has little effect on the molecular energy. Hence, a shallow minima is obtained (Figure 2b) when the plane of phenyl group is almost perpendicular to the plane of the parent PAH. The molecular energy variation with torsion angle in cations follow a trend similar to their corresponding neutrals.

The values of final optimized phenyl torsion angles are given in Table 1 for both neutrals and cations. The result for neutral biphenyl agrees closely with the torsion angle reported earlier using various methods [53, 54] and also with the internal rotation ( $\sim 44^\circ$ ) between phenyl groups in poly(p-phenylene) [55]. Upon ionization the torsion angle is reduced in all the molecules, with maximum reduction, by a factor of 2, in biphenyl. As the size increases, the change in torsion angle gets smaller upon ionization. This structural change upon ionization becomes negligible in 14-phenylovalene ( $\sim 0.1^\circ$ ). The variation in the torsion angle upon ionization depends on the change in steric interaction due to change in charge distribution on the hydrogen atoms of the parent moiety near the phenyl group. As the cation size increases the additional charge is distributed over a larger number of atoms, so large cations have smaller charge variation from neutrals [46] and hence lesser change in torsion angle. Table 1 also shows optimized energies and the change in energy upon ionization, i.e. removal of one electron. The energy change on ionization is nearly equal for all molecules, but as the molecule size increases the energy change gets slightly smaller.

To select suitable level of DFT theory and the size of the basis set it is important to compare the computed vibrational frequencies with experimental values. The use of B3LYP/4-31G for calculations on PAHs is well established and the vibrational frequencies show good comparison with experimental data [44, 45]. But use of higher basis sets will give better orbital representation leading to accurate and better results. Report on 2-vinyl-anthracene and 9-vinyl-anthracene [25] indicated the suitability of 6-31G(d) basis set for side group substituted PAHs. The computed frequencies need to be scaled for comparison with experimental spectrum and the scale factor depends on the level of theory used [44, 56, 25]. The current report uses 6-31G(d) basis and the two level frequency scaling procedure [25, 57]. For the C-H stretching vibrations computed around  $3000\text{ cm}^{-1}$  the scale factor considered is 0.9603 and for the  $1800 - 500\text{ cm}^{-1}$  range it is 0.9697.

The computed and scaled vibrational frequencies and the corresponding intensities are used to simulate infrared spectrum of each molecule. In each spectrum Lorentzian profile peaks are obtained considering FWHM of  $5\text{ cm}^{-1}$  and the intensities are taken relative to the most intense mode. These spectra for both neutrals and cations are shown in Figures 3 – 12 for the range  $1800 - 500\text{ cm}^{-1}$ . The vertical dotted lines show  $6.2$  and  $7.7\text{ }\mu\text{m}$  AIB positions. The C-H stretch modes in the  $3000\text{ cm}^{-1}$  range fall very close to each other and collocate into a

complex feature in the simulated spectra. These are shown in Figures 13(a - d). The frequencies and corresponding infrared intensities for each molecule and its cation can be obtained upon request.

In general, the spectral features in phenyl-PAHs are not very different from plain PAHs, even the spectral change upon ionization is similar. For example, in the spectra of neutral phenyl-PAHs the most intense bands correspond to C-H stretch ( $3030\text{ cm}^{-1}$ ) and C-H out-of-plane bend ( $890\text{ cm}^{-1}$ ) modes, but upon ionization, i.e. in cations, the intensity of C-H stretch modes is drastically reduced and the intensity of C-C stretch and C-H in-plane bend modes ( $1600 - 1100\text{ cm}^{-1}$ ) gets enhanced. This variation due to ionization is related to the change in charge distribution around the peripheral hydrogens in plain PAHs [45, 46] and even in PAHs with side groups [20, 26]. The prominent spectral features in  $1800 - 500\text{ cm}^{-1}$  range for each molecule are discussed below individually.

**Biphenyl** - The computed spectrum (Figure 3) compares very well with the reported gas phase infrared spectrum [58] and also with that reported earlier at the same theoretical level [42, 54]. The most intense peak in the neutral molecule is at  $733.0\text{ cm}^{-1}$ , which is a combined peak due to neighbouring C-H out-of-plane modes at  $732.9$  and  $733.2\text{ cm}^{-1}$ . Another strong C-H out-of-plane wag appears at  $692.0\text{ cm}^{-1}$ . Medium intense peaks at  $1612.0$  and  $1486.0\text{ cm}^{-1}$  are due to the C-C stretch and C-H in-plane bend modes. In the spectrum of the cation the most prominent band is the C-C stretch mode at  $1576.4\text{ cm}^{-1}$ .

**1-phenylnaphthalene** - In the spectrum of neutral 1-phenylnaphthalene (Figure 4) the most prominent band lies at  $774.0\text{ cm}^{-1}$ , due to C-H wag motion of three hydrogens in the ring that also contains the phenyl group. This and the band at  $1498.0\text{ cm}^{-1}$  correlate well with the corresponding bands at  $788.8$  and  $1502.5\text{ cm}^{-1}$  in naphthalene [59, 45]. In the neutral there are other C-H out-of-plane wag modes appearing at  $695.9$ ,  $753.6$  and  $794.9\text{ cm}^{-1}$ , while in the cation only one intense band is present related to this mode at  $760.2\text{ cm}^{-1}$ . The cation band is also similar to that observed in plain naphthalene cation at  $767.9\text{ cm}^{-1}$  [45]. The highest intensity mode in cation spectrum is at  $1565.4\text{ cm}^{-1}$ , along with a strong peak at  $1598.1\text{ cm}^{-1}$  and a medium intensity peak near  $1300\text{ cm}^{-1}$ .

**2-phenylnaphthalene** - Four distinct peaks for the C-H out-of-plane bend modes are present at  $692.3$ ,  $753.7$ ,  $765.9$  and  $813.5\text{ cm}^{-1}$ , with the most intense one at  $753.7\text{ cm}^{-1}$  (Figure 5). The  $692.3\text{ cm}^{-1}$  mode is symmetric C-H wag motion in the phenyl side group and the  $813.5\text{ cm}^{-1}$  mode is purely of the naphthalene moiety. For neutral, the C-C stretch mode gives two bands of medium intensity at  $1611.0$  and  $1633.9\text{ cm}^{-1}$  due to the phenyl and naphthalene moiety respectively. Ionization results in a more complex spectrum with several intense features appearing in the  $1100 - 1600\text{ cm}^{-1}$  range. The most intense feature lies at  $1304.1\text{ cm}^{-1}$  due to C-C stretch vibration at the junction of phenyl and the main naphthalene unit. Another

significant peak is at  $1599.7\text{ cm}^{-1}$  due to C-C stretch within the phenyl side group. In both phenylnaphthalenes several modes of the parent PAH remain only slightly disturbed, but the effect of phenyl group is more prominent on substitution at 2<sup>nd</sup> position.

**2-phenylanthracene** - The computed spectrum of neutral (Figure 6) is in good agreement with the reported experimental solid-state spectrum in KBr pellet [60]. Number of intense C-H out-of-plane bend modes appear with contributions from solo, quarto and quintet hydrogens. The prominent peaks are at  $692.7$ ,  $735.1$ ,  $855.7$  and  $881.8\text{ cm}^{-1}$ , with the most intense one due to quarto C-H wag motion at  $735.1\text{ cm}^{-1}$ . The mode at  $881.8\text{ cm}^{-1}$  is due to solo C-H wag motion. These quarto and solo modes correlate well with the corresponding bands at  $734.5$  and  $891.4\text{ cm}^{-1}$  in anthracene [45]. The  $692.7\text{ cm}^{-1}$  peak corresponds to C-H wag in phenyl group and the  $855.7\text{ cm}^{-1}$  peak is due to mixing of phenyl C-H wag motion and solo C-H wag motion. There are also two moderate intensity peaks at  $1609.3$  and  $1630.0\text{ cm}^{-1}$  due to C-C stretch motion in phenyl unit and in anthracene unit respectively.

Upon ionization the quarto and solo modes are blue shifted by  $12.7$  and  $27.4\text{ cm}^{-1}$ , respectively, just as in plain anthracene molecule [29]. In the spectrum of cation the strongest band corresponds to the C-C stretch motion in anthracene unit at  $1538.0\text{ cm}^{-1}$ . The strong band at  $1588.2\text{ cm}^{-1}$  is due to C-C stretch motion in both anthracene and phenyl moieties. Other prominent peaks present at  $1184.4$  and  $1365.4\text{ cm}^{-1}$  arise due to C-C stretch and C-H in-plane bend motion in anthracene unit.

**9-phenylanthracene** - The computed spectrum of neutral 9-phenylanthracene (Figure 7) matches well with the reported gas phase infrared spectrum [61]. The most intense peak at  $731.0\text{ cm}^{-1}$  is due to C-H out-of-plane bend motion of quarto hydrogens and correlates well with the corresponding band at  $734.5\text{ cm}^{-1}$  in anthracene [45]. This mode is unaffected even with side group position as it is at the same position in 2-phenylanthracene. Other intense features due to C-H wag motions appear at  $694.3$ ,  $747.7$  and  $876.1\text{ cm}^{-1}$ . The  $694.3$  and  $747.7\text{ cm}^{-1}$  modes correspond to the C-H out-of-plane motion in the phenyl unit while the  $876.1\text{ cm}^{-1}$  mode is due to solo C-H out-of-plane motion.

Upon ionization the  $694.3$  and  $747.7\text{ cm}^{-1}$  modes are nearly unaltered and the quarto and solo C-H wag modes are blue shifted by  $12.5\text{ cm}^{-1}$  and  $37.0\text{ cm}^{-1}$ , respectively. In the cation, the peak at  $1331.2\text{ cm}^{-1}$  is strongest. This peak results from two close modes, one at  $1329.8\text{ cm}^{-1}$ , attributed to the C-C stretch and C-H in-plane bends motion in both anthracene and phenyl units, and the other at  $1332.6\text{ cm}^{-1}$  due to C-C stretch vibration at the junction of phenyl and the main anthracene unit. The band at  $1196.8\text{ cm}^{-1}$  correlates with the band at  $1188.6\text{ cm}^{-1}$  in plain anthracene [59]. An interesting strong feature at  $1584.4\text{ cm}^{-1}$  corresponds

to C-C stretch motion in both anthracene and phenyl units.

**1-phenylpyrene** - The neutral 1-phenylpyrene spectrum (Figure 8) has a prominent feature at  $843.9\text{ cm}^{-1}$  due to C-H wag in pyrene. This mode is relic of the strong feature at  $850\text{ cm}^{-1}$  in plain pyrene [46]. The other strong peak at  $696.4\text{ cm}^{-1}$  is due to the C-H out-of-plane wag motion of phenyl group hydrogens. This mode corresponds to the strongest peak in the spectrum of phenyl radical observed at  $706\text{ cm}^{-1}$  [32]. The cation spectrum has strong C-C stretch features, at  $1566.1\text{ cm}^{-1}$  due to the pyrene unit and a band at  $1592.4\text{ cm}^{-1}$  due to the phenyl group. The vibration of C-C bond at the junction of phenyl and pyrene moiety contributes to the peak at  $1262.4\text{ cm}^{-1}$ .

**2-phenylpyrene** - There are a number of intense features in both neutral and cation (Figure 9). In the neutral, besides several C-H out-of-plane modes between  $900\text{--}650\text{ cm}^{-1}$ , there are two strong peaks at  $1611.2$  and  $1601.1\text{ cm}^{-1}$ . These features belong to C-C stretch within the phenyl side group and pyrene moiety respectively. The relative intensity of the band at  $1611.2\text{ cm}^{-1}$  is reduced in cation. The change in the relative intensity of this mode in the cation is not related to ionization, it is due to strong enhancement of intrinsic intensity of other modes in this frequency range upon ionization. The value of absolute intensity of this feature is  $0.36\text{ Debye}^2/\text{AMU}\text{ \AA}^2$  in neutral and is  $0.33\text{ Debye}^2/\text{AMU}\text{ \AA}^2$  in the cation. The strong peaks at  $874.8$  and  $828.2\text{ cm}^{-1}$  correspond to the C-H wag motion in the pyrene unit. While the intense peak at  $693.3\text{ cm}^{-1}$  is due to the C-H out-of-plane wag motion of phenyl group hydrogens and the peaks at  $741.0$  and  $763.5\text{ cm}^{-1}$  arise from the C-H out-of-plane vibrations in both units. These three modes remain unaffected in the cation at  $691.6$ ,  $734.1$  and  $758.7\text{ cm}^{-1}$ . The most intense band in the cation spectrum, however, is at  $1531.2\text{ cm}^{-1}$  with a companion at  $1548.8\text{ cm}^{-1}$ , both due to the C-C stretch vibrations within the pyrene unit.

**4-phenylpyrene** - The spectral features in 4-phenylpyrene (Figure 10) are close to those in 1-phenylpyrene. The neutral exhibits a strong peak at  $825.5\text{ cm}^{-1}$  attributed to C-H out-of-plane wag in the pyrene unit. Other C-H wag modes appear at  $696.6$ ,  $716.6$  and  $866.6\text{ cm}^{-1}$ . In  $1600\text{ cm}^{-1}$  range medium intensity C-C stretch modes peak at  $1598.4$  and  $1609.8\text{ cm}^{-1}$ . In the cation the most intense band is at  $1279.4\text{ cm}^{-1}$ . There is a strong C-C stretch mode at  $1592.3\text{ cm}^{-1}$ . Another strong feature at  $1554.9\text{ cm}^{-1}$  is due to pyrene moiety C-H in-plane bend mode. Comparing the spectra of three different substituent positions of phenyl group in pyrene, it is observed that the substitution at  $2^{nd}$  position shows greater effect and enhances the infrared activity of several modes.

**1-phenylcoronene** - The spectrum of neutral and cation (Figure 11) are very similar to those of plain coronene [46]. In neutral a prominent feature is at  $846.3\text{ cm}^{-1}$ , due to the C-H out-of-plane wag motion of the coronene duo hydrogens. The effect of phenyl substitution results in additional medium intensity

mode at  $884.6\text{ cm}^{-1}$ . The cation spectrum consist of some intense features in the range  $1100 - 1600\text{ cm}^{-1}$ , with the most prominent band at  $1571.9\text{ cm}^{-1}$  corresponding to C-C stretch and C-H in-plane bending vibrations in coronene. The presence of phenyl group does induce additional features at  $1582.9$  and  $1593.3\text{ cm}^{-1}$ .

**14-phenylovalene** - The spectrum of neutral 14-phenylovalene, like neutral ovalene [46], has two intense peaks for C-H out-of-plane bend vibrations at  $835.8$  and  $870.3\text{ cm}^{-1}$ , corresponding respectively to the duo and solo hydrogens (Figure 12). Additional peaks of moderate intensity are present at  $695.2$  and  $705.7\text{ cm}^{-1}$  due to phenyl C-H wag motions. For neutral, the  $1200 - 1600\text{ cm}^{-1}$  region has four medium intensity features at  $1235.2$ ,  $1327.5$ ,  $1609.9$  and  $1629.7\text{ cm}^{-1}$ . The  $1235.2\text{ cm}^{-1}$  mode is mainly C-H in-plane bending, while the  $1327.5\text{ cm}^{-1}$  feature is due to aromatic C-C stretch vibrations in ovalene unit and stretching of the single C-C bond that joins the phenyl and ovalene units. In cation, intense peaks appear at  $1227.8$ ,  $1322.0$ ,  $1341.0$ ,  $1544.7$  and  $1590.3\text{ cm}^{-1}$  along with several moderate intensity features. The strongest peak at  $1590.3\text{ cm}^{-1}$  corresponds to C-C stretch vibrations in ovalene moiety.

**The C-H stretch mode** features are of significance only in the neutral molecules as in the cations these modes are more than an order of magnitude less intense. In Figure 13, the intensity scale for cations is expanded so that the C-H stretch features may be visible. The frequency position in cations is slightly blue shifted with respect to the neutrals. As the phenyl group is also aromatic all hydrogens have similar bonding and give rise to a collective feature, with multiple peaks. Astronomical observations reveal that the  $3.3\text{ }\mu\text{m}$  ( $3030\text{ cm}^{-1}$ ) band is accompanied by a plateau and sub-features [62]. The profile and position of the peaks observed along different astronomical objects is different. This difference is attributed to the different size and peripheral structure of PAHs [63, 62].

In neutral molecules with phenyl group substituted at  $1^{st}$  position, an interesting peak near  $3110\text{ cm}^{-1}$  ( $3.2\text{ }\mu\text{m}$ ) is observed. This mode corresponds to the motion of hydrogen that is asymmetrically placed with respect to the phenyl group. This mode has enhanced frequency possibly due to the hindered hydrogen motion. Although 4-phenylpyrene has a similar asymmetry, as reflected in its similar energy – angle variation (Figure 2b) it does not exhibit this enhanced feature. This may be because in 4-phenylpyrene the position and inclination of phenyl group makes the surrounding hydrogens spaced more at ease as compared to that in 1-substitution. The solo position phenyl substituted molecules (14-phenylovalene and 9-phenylanthracene) have energy – angle variation similar to that in  $1^{st}$  position substituted phenyl PAHs (Figure 2b). But, only 14-phenylovalene exhibits a peak near  $3110\text{ cm}^{-1}$  which corresponds to the vibrational motions in symmetrically placed hydrogen atoms with respect to the phenyl group.

## 3 Discussion

The possibility of phenyl substituted PAHs in the ISM is indicated via combustion pyrolysis of simple aromatic molecules [40, 38, 43, 41, 35, 42, 64]. Like unsubstituted plain PAHs, phenyl substituted PAHs also exhibit features near the AIB regions. But these species introduce additional interesting features in their infrared spectra, that need to be examined for suitable incorporation in composite PAH-AIB models. In this section, variation in peak position and intensity of C-H out-of-plane and C-C stretch vibrational bands are analysed. Attempt is made to identify any correlation of the variations with different shapes, sizes, and ionization of studied phenyl-PAHs.

### 3.1 C-H out-of-plane vibrations

The peak positions of prominent C-H out-of-plane features for neutrals and corresponding cations of all molecules are listed in the Table 2. It is observed that generally the C-H out-of-plane vibrations in the phenyl moiety, marked with superscript 'a', and those in the parent plain PAHs can be distinctly identified. Therefore, the two types of features are discussed separately.

#### 3.1.1 Phenyl C-H wag

The quintet C-H present in the phenyl moiety produces out-of-plane vibrational bands in  $692 - 706 \text{ cm}^{-1}$  ( $14.5 - 14.1 \text{ }\mu\text{m}$ ) and  $730 - 770 \text{ cm}^{-1}$  ( $13.7 - 13.0 \text{ }\mu\text{m}$ ) regions [29]. A common feature in all studied neutral systems is the peak near  $695 \text{ cm}^{-1}$  (Table 2). Similar feature has been reported in neutral biphenyl and polyphenyls [42]. This mode is attributed to the in phase out-of-plane vibration of all five phenyl group hydrogens. Only in neutral 14-phenylovalene, instead of a single peak there is a doublet with peaks at  $695.2$  and  $705.7 \text{ cm}^{-1}$ .

The band position and intensity of this feature is plotted against the size of the phenyl-PAH for neutrals and their corresponding cations in Figure 14. As the PAH size increases the frequency of this mode in neutrals is nearly unaltered i.e., the mode is independent of the size of the molecule. Upon ionization the mode is red shifted, with largest shift for biphenyl ( $65 \text{ cm}^{-1}$ ). The red shift decreases with the size of the PAH and it is negligible in 14-phenylovalene. The shift in the band position in cations can be attributed to the change in fractional charge on the phenyl hydrogen atoms, as the PAH size increases the change in charge reduces [45, 46].

The absolute intensity of this quintet phenyl C-H wag mode is maximum for biphenyl, it decreases gradually with PAH size and is minimum for 14-phenylovalene (Figure 14). Ionization results in the increase of absolute intensity of this mode,

except in 4-phenylpyrene and 14-phenylvalene. The fractional change in absolute intensity upon ionization is less than 0.50 for this mode (Table 2).

The higher frequency phenyl C-H wag mode in the 730 – 770  $\text{cm}^{-1}$  region corresponds to the C-H out-of-plane vibrations of the front three hydrogens in the phenyl moiety. This mode is clearly observed in all except 2<sup>nd</sup> substituted phenyl-PAHs (Table 2). The parent PAH's quarto C-H wag and the tail of the trio C-H wag modes, being in the same frequency range, get mixed with the phenyl quintet C-H modes. Upon ionization, this feature shows very small shift ( $\Delta\nu < 8 \text{ cm}^{-1}$ ) except in biphenyl, and the absolute intensity of the mode is maximum in biphenyl cation (Table 2).

### 3.1.2 C-H wag in parent unit

The substitution of phenyl group has little effect on the main C-H out-of-plane modes of the parent PAH. A comparison of main peaks of the phenyl-PAH in C-H out-of-plane bend region to the features in corresponding parent PAH is presented in Table 3. The modes related to C-H wag in the parent unit of phenyl-PAHs are blue shifted upon ionization, just as in plain PAHs [29, 47]. In contrast the quintet phenyl C-H wag modes are normally red shifted upon ionization. The quarto and trio modes of parent unit that have mixed contributions from the phenyl quintet C-H out-of-plane motion show both blue and red shifting, depending on the fraction of mixing.

The quarto C-H wag exists in single layered plain PAHs. Besides the features similar to those in parent PAHs, additional features due to interaction and mixing of phenyl C-H wag appear in phenylnaphthalenes at 774.0, 753.7 and 765.9  $\text{cm}^{-1}$ . Upon ionization, the 774.0  $\text{cm}^{-1}$  peak of 1-phenylnaphthalene and 765.9  $\text{cm}^{-1}$  peak of 2-phenylnaphthalene shift redwards, while the 753.7  $\text{cm}^{-1}$  peak of 2-phenylnaphthalene is blue shifted.

The trio C-H out-of-plane vibrations present in phenylpyrenes also have mixed contributions of phenyl C-H out-of-plane vibrations. These modes fall in the range 741 – 764  $\text{cm}^{-1}$  (Table 3). The mixing of modes does not much affect the peak positions and only slightly alter the intensity patterns.

The duo C-H wag modes show split in peaks but fall in the range similar to corresponding plain PAHs [29, 46]. These modes are intense features and peak between 828 – 875  $\text{cm}^{-1}$ . The solo C-H wag modes present at 881.8, 876.1 and 870.3  $\text{cm}^{-1}$  in 2-phenylanthracene, 9-phenylanthracene and 14-phenylvalene, respectively, are akin to the corresponding parent PAH features and show similar blue shift in the cations [29, 45, 46].

### 3.2 The C-C stretch modes

The strong and intense features associated with C-C stretch vibrations appear normally in PAH cations. The addition of phenyl group introduces a significant peak of the *phenyl group C-C stretch*, in the astrophysically relevant  $1600\text{ cm}^{-1}$  ( $6.2\text{ }\mu\text{m}$ ) spectral region, except in cations of 14-phenylovalene and 2-phenylpyrene. The frequency position of the significant peaks in each molecule are shown in Figure 15. The phenyl group vibrations in cations are marked with ‘ $\times$ ’. Except in biphenyl, these modes lie well inside the  $6.2\text{ }\mu\text{m}$  AIB region, demarcated by horizontal lines in the figure. In 2-phenylpyrene it is the neutral that shows a significant peak in this spectral region, marked by ‘ $\triangle$ ’ symbol. These may be considered favourable results, suitable for incorporation in astrophysical models. But in all cases, there is a strong feature mostly due to C-C stretch in the parent aromatic moiety, marked as ‘o’ in the figure. In all molecules this is the more intense mode compared to the higher frequency phenyl group C-C stretch mode, except in 2-phenylnaphthalene, where it’s intensity is slightly less. This parent PAH C-C stretch is very much affected by the position of phenyl group substitution. The phenyl substitution at 1 position enhances this plain PAH mode to around  $1570\text{ cm}^{-1}$  ( $6.3\text{ }\mu\text{m}$ ), while phenyl substitution at other positions vary randomly from molecule to molecule. The two solo position phenyl substitutions, as in 9-phenylanthracene and 14-phenylovalene, show large enhancement in the mode bringing it within the  $6.2\text{ }\mu\text{m}$  AIB region.

### 3.3 Astrophysical significance

The infrared emission bands observed from diverse astrophysical objects depend on the excitation and internal conversion mechanisms in possible PAHs and result from transitions in higher vibrational levels. This may cause the emission features to be broader and slightly ( $\sim 10\text{ cm}^{-1}$ ) red shifted with respect to gas phase absorption bands. The exact magnitude of this effect vary between molecules and between vibrational modes and both are less than the natural line width of the interstellar emitters, i.e.  $\sim 30\text{ cm}^{-1}$  [65, 66, 67]. There are few laboratory emission studies available which show no drastic changes between emission and absorption bands [68, 69] and are also in good agreement with theoretical calculations. Therefore, the spectral data presented here do not include correction for the redshift expected between the calculated absorption peaks and the emission frequencies of vibrationally excited PAHs. Comparison of interstellar IR spectra with the calculated absorption spectra could give an idea about the PAH type which may contribute in infrared emission models [70] of different astrophysical sites.

The astronomical emission bands in  $10 - 15\text{ }\mu\text{m}$  range arise from the C-H out-

of-plane bending vibrations [30]. The intensities and positions of various peaks for these features depend on the number of adjacent hydrogen atoms on the periphery of the PAH ring [29]. The frequency position of solo C-H wag is highest and is respectively lowered for duo, trio, quarto, and quintet C-H wags. While the solo and duo C-H out-of-plane vibrations of parent PAHs remain unmodified in phenyl-PAHs, there are additional features due to quintet C-H. Thus, astrophysical observation of any emission feature at lower frequencies may indicate phenyl substitution. The quintet C-H out-of-plane vibrations in phenyl group contribute to peaks in two regions,  $692 - 706 \text{ cm}^{-1}$  ( $14.4 - 14.1 \text{ }\mu\text{m}$ ) and  $770 - 730 \text{ cm}^{-1}$  ( $13.0 - 13.7 \text{ }\mu\text{m}$ ). The quintet features for neutrals lie near  $695 \text{ cm}^{-1}$  ( $14.4 \text{ }\mu\text{m}$ ) and except in biphenyl the cations show small red shift (Section 3.1.1, Figure 14). The position of this mode is independent of the size and shape of phenyl-PAHs and is also unaffected by the position of phenyl group attachment. A feature between  $14.2 - 14.3 \text{ }\mu\text{m}$  is observed in a variety of sources [30, 18, 19], which may be the quintet C-H wag contribution from phenyl-PAHs. Therefore, the environments of these objects may contain phenyl-PAHs and must be included in emission models.

Another weak infrared emission band at  $13.5 \text{ }\mu\text{m}$  ( $741 \text{ cm}^{-1}$ ), observed in different astrophysical sites [30], falls in the region of the other quintet C-H out-of-plane feature, i.e.,  $13.0 - 13.7 \text{ }\mu\text{m}$  range. This quintet phenyl C-H wag mode is mixed with quartet or trio C-H wags in phenyl-PAHs (section 3.1.1). Among the phenyl-PAHs in the present work, the phenylpyrenes and neutral 2-phenylpyrene, in particular, show good match with the feature at  $741.0 \text{ cm}^{-1}$  ( $13.5 \text{ }\mu\text{m}$ ) (Table 3). This is a trio C-H wag that has mixed contribution from phenyl C-H out-of-plane bending. There is negligible red shift of this feature upon ionization. The mixing of quintet and trio/quarto C-H out-of-plane modes in phenyl-PAHs may provide prominent features in this spectral range, so more pyrene like compact PAHs with phenyl side groups need to be studied.

Astrophysical objects exhibiting the  $14.2 \text{ }\mu\text{m}$  feature generally show class A type  $6.2 \text{ }\mu\text{m}$  AIB (peak in  $6.20 - 6.22 \text{ }\mu\text{m}$ ) [14]. But some late type objects, viz. HD 44179 (Post-AGB star), HE 2-113 (Planetary nebulae), IRAS 17047 (Planetary nebulae), with  $14.2 \text{ }\mu\text{m}$  band show class B type  $6.2 \text{ }\mu\text{m}$  AIB (peak in  $6.23 - 6.26 \text{ }\mu\text{m}$ ) [14]. In the present work, all the phenyl-PAH cations except 2-phenylpyrene exhibit a significantly strong peak (Figure 15) giving closer match to class B  $6.2 \text{ }\mu\text{m}$  AIB. In the case of 2-phenylpyrene it is the neutral which gives a strong phenyl C-C stretch peak that is also close to class B  $6.2 \text{ }\mu\text{m}$  AIB. This points towards the possibility of the presence of phenyl-PAHs in the environments of such late type stars. Neutral 2-phenylpyrene is also interesting due to additional strong modes in this range. While the  $1432 \text{ cm}^{-1}$  ( $6.98 \text{ }\mu\text{m}$ ) peak falls close to a feature  $\sim 6.9 \text{ }\mu\text{m}$ , observed in protoplanetary nebulae and cool objects [71, 72], the  $1501 \text{ cm}^{-1}$  ( $6.66 \text{ }\mu\text{m}$ ) peak can correspond to observed sub-feature along IRAS

18434-0242 [73] and in H II region-like and seyfert 2 galaxies [74]. The  $1500\text{ cm}^{-1}$  peak is also present in neutral 2-phenylnaphthalene.

The substitution of phenyl side group on PAHs does shift the C-C stretch mode of parent PAH towards higher frequencies that depend on the site of phenyl substitution. Astrophysical observations do not show any strong feature on the red side of the  $6.2\text{ }\mu\text{m}$  AIB and specific object spectrum needs to be examined more closely for possible fitting of a broadened Class C AIB feature. In 9-phenylanthracene and 14-phenylovalene, where phenyl substitution is at solo position, there is large enhancement in the mode bringing it within the  $6.2\text{ }\mu\text{m}$  AIB region (Figure 15).

The current NASA PAH data base [57] contains a large variety of PAHs but PAHs with phenyl side group are not considered. The comparison with observations does indicate towards the possibility of phenyl-PAHs in the ISM. In particular species with substitution at  $2^{nd}$  position are relatively stable and compact 2-phenylpyrene type or solo substituted species appear to be more promising.

## 4 Conclusions

Structural analysis of a number of neutral and positively charged phenyl-PAHs is performed and their corresponding infra-red spectra are examined. Generally, the infra-red spectral features of phenyl-PAH neutrals and cations are similar to those in their corresponding plain PAHs. But there are a number of bands that are peculiar to phenyl-PAHs.

The main conclusions of the study are summarized below:

- The variation of the energy of optimized molecular structure at different torsion angles, for the phenyl group, shows that the substitution of phenyl at  $2^{nd}$  position gives more stable specie than the substitution of phenyl at other positions in different PAH molecules.
- The quintet C-H out-of-plane vibrations, possible only in phenyl group, lie near  $695\text{ cm}^{-1}$  ( $14.4\text{ }\mu\text{m}$ ) in all the studied phenyl-PAHs and is independent of the molecule's shape, size and position of phenyl substitution. This feature compares well with the observed emission feature between  $14.2 - 14.3\text{ }\mu\text{m}$  in diverse astrophysical objects [30, 18, 19].
- The quintet mixed with quartet or trio C-H out-of-plane bending modes produce minor band in  $13.0 - 13.7\text{ }\mu\text{m}$  range. Among the studied phenyl-PAHs, phenylpyrenes and neutral 2-phenylpyrene in particular, show good match with the observed astrophysical feature at  $741.0\text{ cm}^{-1}$  ( $13.5\mu\text{m}$ ) [30].
- A significantly strong peak due to phenyl C-C stretch (Figure 15), giving close match to class B  $6.2\text{ }\mu\text{m}$  AIB, is exhibited in all phenyl-PAH cations.

In the case of 2-phenylpyrene it is the neutral which gives a strong phenyl C-C stretch peak that is also close to class B 6.2  $\mu\text{m}$  AIB. This points towards the presence of phenyl-PAHs in the environments of late type stars, which exhibit class B 6.2  $\mu\text{m}$  AIB.

- Neutral 2-phenylpyrene is also interesting due to additional strong modes in the 1400 - 1500  $\text{cm}^{-1}$  range. While the 1432  $\text{cm}^{-1}$  (6.98  $\mu\text{m}$ ) peak falls close to a feature  $\sim 6.9$   $\mu\text{m}$ , observed in protoplanetary nebulae and cool objects [71, 72], the 1501  $\text{cm}^{-1}$  (6.66  $\mu\text{m}$ ) peak can correspond to observed sub-feature along IRAS 18434-0242 [73] and in HII region like and seyfert 2 galaxies [74]. This mode is also present in neutral 2-phenylnaphthalene.
- The substitution of phenyl side group on PAHs also shift the C-C stretch mode of parent PAH towards higher frequencies that depend on the position of phenyl substitution. The shift in solo position substituted phenyl-PAHs is large enough to reach the 6.2  $\mu\text{m}$  AIB region.

On the basis of structural and spectral analysis, the possibility of phenyl-PAHs in carbon rich cool circumstellar shells is indicated. Medium sized compact phenyl-PAHs can form in high-density regions and shocks [38, 43] that are possible in protoplanetary circumstellar shells. A bottom-up scenario for the formation of PAHs is suggested [75] in dense photodissociation regions (PDRs) of planetary and protoplanetary nebulae. Hence, the PAH database, used to model AIB emission features for specific astrophysical objects, must include phenyl-PAHs.

## 5 Acknowledgment

Authors acknowledge the use of computing and library facilities of the Inter-University Centre for Astronomy and Astrophysics, Pune, India. A. Maurya acknowledges the CSIR-HRDG New Delhi for its RA fellowship.

## References

- [1] A. Leger, J. L. Puget, Identification of the 'unidentified' IR emission features of interstellar dust?, *Astron. Astrophys.* 137 (1984) L5–L8.
- [2] L. J. Allamandola, A. G. G. M. Tielens, J. R. Barker, Polycyclic aromatic hydrocarbons and the unidentified infrared emission bands - Auto exhaust along the Milky Way, *Astrophys. J. Lets.* 290 (1985) L25–L28. doi:10.1086/184435.

- [3] A. G. G. M. Tielens, Interstellar Polycyclic Aromatic Hydrocarbon Molecules, *Annu. Rev. Astron. Astrophys.* 46 (2008) 289–337. doi:10.1146/annurev.astro.46.060407.145211.
- [4] A. Li, Spitzer’s perspective of polycyclic aromatic hydrocarbons in galaxies, *Nature Astronomy* 4 (4) (2020) 339–351. doi:10.1038/s41550-020-1051-1. URL <https://doi.org/10.1038/s41550-020-1051-1>
- [5] M. Cohen, A. G. G. M. Tielens, J. Bregman, F. C. Witteborn, D. M. Rank, L. J. Allamandola, D. Wooden, M. Jourdain de Muizon, The infrared emission bands. III - Southern IRAS sources, *Astrophys. J.* 341 (1989) 246–269. doi:10.1086/167489.
- [6] D. A. Beintema, M. E. van den Ancker, F. J. Molster, L. B. F. M. Waters, A. G. G. M. Tielens, C. Waelkens, T. de Jong, T. de Graauw, K. Justtanont, I. Yamamura, A. Heras, F. Lahuis, A. Salama, The rich spectrum of circumstellar PAHs., *Astron. Astrophys.* 315 (1996) L369–L372.
- [7] D. Lutz, H. W. W. Spoon, D. Rigopoulou, A. F. M. Moorwood, R. Genzel, The Nature and Evolution of Ultraluminous Infrared Galaxies: A Mid-Infrared Spectroscopic Survey, *Astrophys. J. Lett.* 505 (1998) L103–L107. arXiv:astro-ph/9806270, doi:10.1086/311614.
- [8] A. Sajina, L. Yan, L. Armus, P. Choi, D. Fadda, G. Helou, H. Spoon, Spitzer Mid-Infrared Spectroscopy of Infrared Luminous Galaxies at  $z \sim 2$ . II. Diagnostics, *Astrophys. J.* 664 (2) (2007) 713–737. arXiv:0704.1765, doi:10.1086/519446.
- [9] M. Matsuura, J. M. DeÂ Buizer, R. G. Arendt, E. Dwek, M. J. Barlow, A. Bevan, P. Cigan, H. L. Gomez, J. Rho, R. Wesson, P. Bouchet, J. Danziger, M. Meixner, SOFIA mid-infrared observations of Supernovaâ€™1987A in 2016 â€“ forward shocks and possible dust re-formation in the post-shocked region, *Monthly Notices of the Royal Astronomical Society* 482 (2) (2018) 1715–1723. doi:10.1093/mnras/sty2734. URL <https://doi.org/10.1093/mnras/sty2734>
- [10] M. Lacy, A. Sajina, Active galactic nuclei as seen by the spitzer space telescope, *Nature Astronomy* 4 (4) (2020) 352–363. doi:10.1038/s41550-020-1071-x. URL <https://doi.org/10.1038/s41550-020-1071-x>
- [11] A. G. G. M. Tielens, The molecular universe, *Rev. Mod. Phys.* 85 (2013) 1021–1081. doi:10.1103/RevModPhys.85.1021. URL <https://link.aps.org/doi/10.1103/RevModPhys.85.1021>

- [12] L. J. Allamandola, A. G. G. M. Tielens, J. R. Barker, Interstellar polycyclic aromatic hydrocarbons - The infrared emission bands, the excitation/emission mechanism, and the astrophysical implications, *Astrophys. J. Supp. Ser.* 71 (1989) 733–775. doi:10.1086/191396.
- [13] A. Leger, L. D’Hendecourt, D. Defourneau, Physics of IR emission by interstellar PAH molecules, *Astron. Astrophys.* 216 (1989) 148–164.
- [14] E. Peeters, S. Hony, C. Van Kerckhoven, A. G. G. M. Tielens, L. J. Allamandola, D. M. Hudgins, C. W. Bauschlicher, The rich 6 to 9  $\mu$ m spectrum of interstellar PAHs, *Astron. Astrophys.* 390 (2002) 1089–1113. arXiv:astro-ph/0205400, doi:10.1051/0004-6361:20020773.
- [15] B. van Diedenoven, E. Peeters, C. Van Kerckhoven, S. Hony, D. M. Hudgins, L. J. Allamandola, A. G. G. M. Tielens, The Profiles of the 3-12 Micron Polycyclic Aromatic Hydrocarbon Features, *Astrophys. J.* 611 (2004) 928–939. arXiv:astro-ph/0405098, doi:10.1086/422404.
- [16] A. Pathak, S. Rastogi, Modeling the interstellar aromatic infrared bands with co-added spectra of PAHs, *Astron. Astrophys.* 485 (2008) 735–742. arXiv:0804.2555, doi:10.1051/0004-6361:20066618.
- [17] E. Peeters, J. Bauschlicher, Charles W., L. J. Allamandola, A. G. G. M. Tielens, A. Ricca, M. G. Wolfire, The PAH Emission Characteristics of the Reflection Nebula NGC 2023, *Astrophys. J.* 836 (2) (2017) 198. arXiv:1701.06585, doi:10.3847/1538-4357/836/2/198.
- [18] H. Andrews, C. Boersma, M. W. Werner, J. Livingston, L. J. Allamandola, A. G. G. M. Tielens, PAH Emission at the Bright Locations of PDRs: the grandPAH Hypothesis, *Astrophys. J.* 807 (1) (2015) 99. doi:10.1088/0004-637X/807/1/99.
- [19] C. Boersma, J. Bregman, L. J. Allamandola, The Charge State of Polycyclic Aromatic Hydrocarbons across a Reflection Nebula, an H II Region, and a Planetary Nebula, *Astrophys. J.* 858 (2) (2018) 67. doi:10.3847/1538-4357/aabcbe.
- [20] S. R. Langhoff, C. W. Bauschlicher, D. M. Hudgins, S. A. Sandford, L. J. Allamandola, Infrared spectra of substituted polycyclic aromatic hydrocarbons, *The Journal of Physical Chemistry A* 102 (9) (1998) 1632–1646. arXiv:http://pubs.acs.org/doi/pdf/10.1021/jp9731563, doi:10.1021/jp9731563. URL http://pubs.acs.org/doi/abs/10.1021/jp9731563

- [21] L. W. Beegle, T. J. Wdowiak, J. G. Harrison, Hydrogenation of polycyclic aromatic hydrocarbons as a factor affecting the cosmic 6.2 micron emission band, *Spectrochimica Acta Part A: Molecular and Biomolecular Spectroscopy* 57 (2001) 737–744.
- [22] M. Buragohain, A. Pathak, P. Sarre, N. K. Gour, Interstellar dehydrogenated PAH anions: vibrational spectra, *Monthly Notices of the Royal Astronomical Society* 474 (2018) 4594–4602. [arXiv:1711.09505](#), [doi:10.1093/mnras/stx3060](#).
- [23] M. Tsuge, M. Bahou, Y.-J. Wu, L. Allamandola, Y.-P. Lee, The Infrared Spectrum of Protonated Ovalene in Solid Para-Hydrogen and its Possible Contribution to Interstellar Unidentified Infrared Emission, *Astrophys. J.* 825 (2) (2016) 96. [doi:10.3847/0004-637X/825/2/96](#).
- [24] D. M. Hudgins, C. W. Bauschlicher, Jr., L. J. Allamandola, Variations in the Peak Position of the 6.2  $\mu\text{m}$  Interstellar Emission Feature: A Tracer of N in the Interstellar Polycyclic Aromatic Hydrocarbon Population, *Astrophys. J.* 632 (2005) 316–332. [doi:10.1086/432495](#).
- [25] A. Maurya, S. Rastogi, G. Rouillé, F. Huisken, T. Henning, Experimental and Theoretical Study on the Infrared Spectroscopy of Astrophysically Relevant Polycyclic Aromatic Hydrocarbon Derivatives 2- and 9-Vinyanthracene, *Astrophys. J.* 755 (2012) 120. [arXiv:1207.0738](#), [doi:10.1088/0004-637X/755/2/120](#).
- [26] A. Maurya, S. Rastogi, Vibrational spectroscopic study of vinyl substituted polycyclic aromatic hydrocarbons, *Spectrochimica Acta Part A: Molecular and Biomolecular Spectroscopy* 151 (2015) 1 – 10. [doi:https://doi.org/10.1016/j.saa.2015.06.069](#).  
URL <http://www.sciencedirect.com/science/article/pii/S1386142515300093>
- [27] T. Pino, E. Dartois, A. T. Cao, Y. Carpentier, T. Chamaillé, R. Vasquez, A. P. Jones, L. D’Hendecourt, P. Bréchnac, The 6.2  $\mu\text{m}$  band position in laboratory and astrophysical spectra: a tracer of the aliphatic to aromatic evolution of interstellar carbonaceous dust, *Astron. Astrophys.* 490 (2) (2008) 665–672. [doi:10.1051/0004-6361:200809927](#).
- [28] H. Álvaro Galué, G. Díaz Leines, Origin of spectral band patterns in the cosmic unidentified infrared emission, *Phys. Rev. Lett.* 119 (2017) 171102. [doi:10.1103/PhysRevLett.119.171102](#).  
URL <https://link.aps.org/doi/10.1103/PhysRevLett.119.171102>

- [29] D. M. Hudgins, L. J. Allamandola, Interstellar PAH emission in the 11–14 micron region: New insights from laboratory data and a tracer of ionized pahs, *Astrophys. J. Lett.* 516 (1) (1999) L41–L44. doi:10.1086/311989. URL <https://doi.org/10.1086/311989>
- [30] S. Hony, C. Van Kerckhoven, E. Peeters, A. G. G. M. Tielens, D. M. Hudgins, L. J. Allamandola, The CH out-of-plane bending modes of PAH molecules in astrophysical environments, *Astron. Astrophys.* 370 (2001) 1030–1043. arXiv:astro-ph/0103035, doi:10.1051/0004-6361:20010242.
- [31] J. Bauschlicher, Charles W., E. Peeters, L. J. Allamandola, The Infrared Spectra of Very Large Irregular Polycyclic Aromatic Hydrocarbons (PAHs): Observational Probes of Astronomical PAH Geometry, Size, and Charge, *Astrophys. J.* 697 (1) (2009) 311–327. arXiv:0903.0412, doi:10.1088/0004-637X/697/1/311.
- [32] A. V. Friderichsen, J. G. Radziszewski, M. R. Nimlos, P. R. Winter, D. C. Dayton, D. E. David, G. B. Ellison, The infrared spectrum of the matrix-isolated phenyl radical, *Journal of the American Chemical Society* 123 (9) (2001) 1977–1988, PMID: 11456819. arXiv:<https://doi.org/10.1021/ja0024338>, doi:10.1021/ja0024338. URL <https://doi.org/10.1021/ja0024338>
- [33] P. Tandon, V. D. Gupta, O. Prasad, S. Rastogi, S. B. Katti, Heat capacity and vibrational dynamics of poly( $\beta$  benzyl-L-aspartate), *Journal of Polymer Science Part B: Polymer Physics* 34 (7) (1996) 1213–1228. doi:10.1002/(SICI)1099-0488(199605)34:7<1213::AID-POLB4>3.0.CO;2-W.
- [34] C. Ngaojampa, S. Namuangruk, Y. Surakhot, V. Promarak, S. Jungsutitwong, N. Kungwan, Influence of phenyl-attached substituents on the vibrational and electronic spectra of meso-tetraphenylporphyrin: A dft study, *Computational and Theoretical Chemistry* 1062 (2015) 1 – 10. doi:<https://doi.org/10.1016/j.comptc.2015.03.009>. URL <http://www.sciencedirect.com/science/article/pii/S2210271X15001152>
- [35] I. Cherchneff, The formation of Polycyclic Aromatic Hydrocarbons in evolved circumstellar environments, in: C. Joblin, A. G. G. M. Tielens (Eds.), *EAS Publications Series*, Vol. 46 of *EAS Publications Series*, 2011, pp. 177–189. arXiv:1010.2703, doi:10.1051/eas/1146019.
- [36] R. J. McMahon, M. C. McCarthy, C. A. Gottlieb, J. B. Dudek, J. F. Stanton, P. Thaddeus, The radio spectrum of the phenyl radical, *The Astrophysical*

Journal Letters 590 (1) (2003) L61.

URL <http://stacks.iop.org/1538-4357/590/i=1/a=L61>

- [37] D. S. N. Parker, F. Zhang, Y. S. Kim, R. I. Kaiser, A. Landera, V. V. Kislov, A. M. Mebel, A. G. G. M. Tielens, Low temperature formation of naphthalene and its role in the synthesis of pahs (polycyclic aromatic hydrocarbons) in the interstellar medium, *Proceedings of the National Academy of Sciences* 109 (1) (2012) 53–58. [arXiv:https://www.pnas.org/content/109/1/53.full.pdf](https://arxiv.org/abs/https://www.pnas.org/content/109/1/53.full.pdf), doi:10.1073/pnas.1113827108.  
URL <https://www.pnas.org/content/109/1/53>
- [38] P. M. Woods, T. J. Millar, A. A. Zijlstra, E. Herbst, The synthesis of benzene in the proto-planetary nebula crl 618, *Astrophys. J. Lets.* 574 (2) (2002) L167.  
URL <http://stacks.iop.org/1538-4357/574/i=2/a=L167>
- [39] B. A. McGuire, A. M. Burkhardt, S. Kalenskii, C. N. Shingledecker, A. J. Remijan, E. Herbst, M. C. McCarthy, Detection of the aromatic molecule benzonitrile (c-c6h5cn) in the interstellar medium, *Science* 359 (6372) (2018) 202–205. [arXiv:http://science.sciencemag.org/content/359/6372/202.full.pdf](https://arxiv.org/abs/http://science.sciencemag.org/content/359/6372/202.full.pdf), doi:10.1126/science.aao4890.  
URL <http://science.sciencemag.org/content/359/6372/202>
- [40] G. M. Badger, J. Novotny, 661. the formation of aromatic hydrocarbons at high temperatures. part xii. the pyrolysis of benzene, *J. Chem. Soc.* (1961) 3400–3402doi:10.1039/JR9610003400.  
URL <http://dx.doi.org/10.1039/JR9610003400>
- [41] B. Shukla, A. Susa, A. Miyoshi, M. Koshi, Role of phenyl radicals in the growth of polycyclic aromatic hydrocarbons, *The Journal of Physical Chemistry A* 112 (11) (2008) 2362–2369. [arXiv:https://doi.org/10.1021/jp7098398](https://arxiv.org/abs/https://doi.org/10.1021/jp7098398), doi:10.1021/jp7098398.  
URL <https://doi.org/10.1021/jp7098398>
- [42] D. Talbi, G. S. Chandler, Theoretical infrared spectra of biphenyl, terphenyls and tetraphenyls for astrophysical purposes, *Journal of Molecular Spectroscopy* 275 (2012) 21–27. doi:10.1016/j.jms.2012.04.008.
- [43] K. Mimura, R. Sugisaki, Shock reactions of carbon-bearing materials and their cosmochemical significance., in: T. S. e. Lee Davison, Yasuyuki Horie (Ed.), *High-Pressure Shock Compression of Solids V: Shock Chemistry with Applications to Meteorite Impacts*, Springer-Verlag New York, 2003, pp. 75–116.

- [44] S. R. Langhoff, Theoretical infrared spectra for polycyclic aromatic hydrocarbon neutrals, cations, and anions, *The Journal of Physical Chemistry* 100 (8) (1996) 2819–2841. [arXiv:http://pubs.acs.org/doi/pdf/10.1021/jp952074g](http://pubs.acs.org/doi/pdf/10.1021/jp952074g), doi:10.1021/jp952074g.  
URL <http://pubs.acs.org/doi/abs/10.1021/jp952074g>
- [45] A. Pathak, S. Rastogi, Computational study of neutral and cationic catacondensed polycyclic aromatic hydrocarbons, *Chemical Physics* 313 (1–3) (2005) 133 – 150. doi:<http://dx.doi.org/10.1016/j.chemphys.2005.01.007>.  
URL <http://www.sciencedirect.com/science/article/pii/S030101040500008X>
- [46] A. Pathak, S. Rastogi, Computational study of neutral and cationic pericondensed polycyclic aromatic hydrocarbons, *Chemical Physics* 326 (2006) 315 – 328. doi:<http://dx.doi.org/10.1016/j.chemphys.2006.02.008>.  
URL <http://www.sciencedirect.com/science/article/pii/S0301010406001170>
- [47] A. Pathak, S. Rastogi, Theoretical infrared spectra of large polycyclic aromatic hydrocarbons, *Spectrochimica Acta Part A: Molecular and Biomolecular Spectroscopy* 67 (3–4) (2007) 898 – 909. doi:<http://dx.doi.org/10.1016/j.saa.2006.09.007>.  
URL <http://www.sciencedirect.com/science/article/pii/S1386142506005270>
- [48] C. W. Bauschlicher, Jr., E. Peeters, L. J. Allamandola, The Infrared Spectra of Very Large, Compact, Highly Symmetric, Polycyclic Aromatic Hydrocarbons (PAHs), *Astrophys. J.* 678 (2008) 316–327. [arXiv:0802.1071](http://arxiv.org/abs/0802.1071), doi:10.1086/533424.
- [49] C. W. Bauschlicher, Jr., C. Boersma, A. Ricca, A. L. Mattioda, J. Cami, E. Peeters, F. Sánchez de Armas, G. Puerta Saborido, D. M. Hudgins, L. J. Allamandola, The NASA Ames Polycyclic Aromatic Hydrocarbon Infrared Spectroscopic Database: The Computed Spectra, *Astrophys. J. Supp. Ser.* 189 (2010) 341–351. doi:10.1088/0067-0049/189/2/341.
- [50] A. Ricca, J. Bauschlicher, Charles W., C. Boersma, A. G. G. M. Tielens, L. J. Allamandola, The Infrared Spectroscopy of Compact Polycyclic Aromatic Hydrocarbons Containing up to 384 Carbons, *Astrophys. J.* 754 (1) (2012) 75. doi:10.1088/0004-637X/754/1/75.
- [51] Rosenberg, Marissa J. F., Berné, Olivier, Boersma, Christiaan, Random mixtures of polycyclic aromatic hydrocarbon spectra match interstellar infrared emission, *Astron. Astrophys.* 566 (2014) L4. doi:10.1051/0004-6361/

201423953.

URL <https://doi.org/10.1051/0004-6361/201423953>

- [52] M. W. GAMESS, Schmidt, K. K. Baldridge, J. A. Boatz, S. T. Elbert, M. S. Gordon, J. H. Jensen, S. Koseki, N. Matsunaga, K. A. Nguyen, S. Su, T. L. Windus, M. Dupuis, J. A. Montgomery, General atomic and molecular electronic structure system, *Journal of Computational Chemistry* 14 (11) (1993) 1347–1363. doi:[10.1002/jcc.540141112](https://doi.org/10.1002/jcc.540141112).  
URL <http://dx.doi.org/10.1002/jcc.540141112>
- [53] O. Bastiansen, S. Samdal, Structure and barrier of internal rotation of biphenyl derivatives in the gaseous state: Part 4. barrier of internal rotation in biphenyl, perdeuterated biphenyl and seven non-ortho-substituted halogen derivatives, *Journal of Molecular Structure* 128 (1) (1985) 115 – 125. doi:[https://doi.org/10.1016/0022-2860\(85\)85044-4](https://doi.org/10.1016/0022-2860(85)85044-4).  
URL <http://www.sciencedirect.com/science/article/pii/0022286085850444>
- [54] K. Furuya, H. Torii, Y. Furukawa, M. Tasumi, Density functional study on the structures and vibrational spectra of the radical anion and cation of biphenyl, *Journal of Molecular Structure: THEOCHEM* 424 (3) (1998) 225 – 235. doi:[https://doi.org/10.1016/S0166-1280\(97\)00153-X](https://doi.org/10.1016/S0166-1280(97)00153-X).  
URL <http://www.sciencedirect.com/science/article/pii/S016612809700153X>
- [55] J. Soto, V. Hernández, J. L. Navarrete, Conformational study and lattice dynamics of poly(p-phenylene: oligomers and polymer, *Synthetic Metals* 51 (1) (1992) 229 – 238. doi:[https://doi.org/10.1016/0379-6779\(92\)90275-N](https://doi.org/10.1016/0379-6779(92)90275-N).  
URL <http://www.sciencedirect.com/science/article/pii/037967799290275N>
- [56] C. W. Bauschlicher, S. R. Langhoff, The calculation of accurate harmonic frequencies of large molecules: the polycyclic aromatic hydrocarbons, a case study, *Spectrochimica Acta Part A: Molecular Spectroscopy* 53 (1997) 1225–1240. doi:[10.1016/S1386-1425\(97\)00022-X](https://doi.org/10.1016/S1386-1425(97)00022-X).
- [57] C. W. Bauschlicher, A. Ricca, C. Boersma, L. J. Allamandola, The NASA ames PAH IR spectroscopic database: Computational version 3.00 with updated content and the introduction of multiple scaling factors, *Astrophys. J. Supp. Ser.* 234 (2) (2018) 32. doi:[10.3847/1538-4365/aaa019](https://doi.org/10.3847/1538-4365/aaa019).
- [58] NIST Chemistry Webbook, Infrared spectra of biphenyl.  
URL <https://webbook.nist.gov/cgi/cbook.cgi?ID=C92524&Type=IR-SPEC&Index=1#IR-SPEC>

- [59] D. M. Hudgins, S. A. Sandford, Infrared spectroscopy of matrix isolated polycyclic aromatic hydrocarbons. 1. pahs containing two to four rings, *The Journal of Physical Chemistry A* 102 (2) (1998) 329–343. arXiv:<https://doi.org/10.1021/jp9834816>, doi:10.1021/jp9834816.  
URL <https://doi.org/10.1021/jp9834816>
- [60] NIST Chemistry Webbook, Infrared spectra of 2-phenylanthracene.  
URL <https://webbook.nist.gov/cgi/inchi?ID=C1981380&Mask=80#IR-Spec>
- [61] NIST Chemistry Webbook, Infrared spectra of 9-phenylanthracene.  
URL <https://webbook.nist.gov/cgi/inchi?ID=C602551&Type=IR-SPEC&Index=0#IR-SPEC>
- [62] E. Maltseva, A. Petrignani, A. Candian, C. J. Mackie, X. Huang, T. J. Lee, A. G. G. M. Tielens, J. Oomens, W. J. Buma, High-resolution ir absorption spectroscopy of polycyclic aromatic hydrocarbons in the 3  $\mu\text{m}$  region: Role of periphery, *The Astrophysical Journal* 831 (1) (2016) 58.  
URL <http://stacks.iop.org/0004-637X/831/i=1/a=58>
- [63] A. Candian, T. H. Kerr, I.-O. Song, J. McCombie, P. J. Sarre, Spatial distribution and interpretation of the 3.3  $\mu\text{m}$  pah emission band of the red rectangle, *Monthly Notices of the Royal Astronomical Society* 426 (1) (2012) 389–397. arXiv:[oup/backfile/content/\\_public/journal/mnras/426/1/10.1111/j.1365-2966.2012.21760.x/2/426-1-389.pdf](http://oup/backfile/content/_public/journal/mnras/426/1/10.1111/j.1365-2966.2012.21760.x/2/426-1-389.pdf), doi:10.1111/j.1365-2966.2012.21760.x.  
URL <http://dx.doi.org/10.1111/j.1365-2966.2012.21760.x>
- [64] L. Zhao, M. B. Prendergast, R. I. Kaiser, B. Xu, U. Ablikim, M. Ahmed, B.-J. Sun, Y.-L. Chen, A. H. H. Chang, R. K. Mohamed, F. R. Fischer, Synthesis of polycyclic aromatic hydrocarbons by phenyl addition - dehydrocyclization: The third way, *Angewandte Chemie International Edition* 58 (48) (2019) 17442–17450. arXiv:<https://onlinelibrary.wiley.com/doi/pdf/10.1002/anie.201909876>, doi:<https://doi.org/10.1002/anie.201909876>.  
URL <https://onlinelibrary.wiley.com/doi/abs/10.1002/anie.201909876>
- [65] J. Brenner, J. R. Barker, Infrared Emission Spectra of Benzene and Naphthalene: Implications for the Interstellar Polycyclic Aromatic Hydrocarbon Hypothesis, *Astrophys. J. Lets.* 388 (1992) L39. doi:10.1086/186325.

- [66] C. Joblin, P. Boissel, A. Leger, L. D'Hendecourt, D. Defourneau, Infrared spectroscopy of gas-phase PAH molecules. II. Role of the temperature., *Astron. Astrophys.* 299 (1995) 835.
- [67] D. J. Cook, R. J. Saykally, Simulated Infrared Emission Spectra of Highly Excited Polyatomic Molecules: A Detailed Model of the PAH-UIR Hypothesis, *Astrophys. J.* 493 (1998) 793. doi:10.1086/305156.
- [68] H.-S. Kim, D. R. Wagner, R. J. Saykally, Single photon infrared emission spectroscopy of the gas phase pyrene cation: Support for a polycyclic aromatic hydrocarbon origin of the unidentified infrared emission bands, *Phys. Rev. Lett.* 86 (2001) 5691–5694. doi:10.1103/PhysRevLett.86.5691.  
URL <https://link.aps.org/doi/10.1103/PhysRevLett.86.5691>
- [69] H.-S. Kim, R. J. Saykally, Single-photon infrared emission spectroscopy of gaseous polycyclic aromatic hydrocarbon cations: A direct test for proposed carriers of the unidentified infrared emission bands, *Astrophys. J. Supp. Ser.* 143 (2) (2002) 455–467. doi:10.1086/343078.
- [70] G. Mulas, G. Mallocci, C. Joblin, D. Toubanc, Estimated IR and phosphorescence emission fluxes for specific polycyclic aromatic hydrocarbons in the Red Rectangle, *Astron. Astrophys.* 446 (2006) 537–549. arXiv: astro-ph/0509586, doi:10.1051/0004-6361:20053738.
- [71] B. J. Hrivnak, K. Volk, S. Kwok, 2-45 Micron Infrared Spectroscopy of Carbon-rich Proto-Planetary Nebulae, *Astrophys. J.* 535 (2000) 275–292. doi:10.1086/308823.
- [72] R. H. Buss, Jr., M. Cohen, A. G. G. M. Tielens, M. W. Werner, J. D. Bregman, F. C. Witteborn, D. Rank, S. A. Sandford, Hydrocarbon emission features in the IR spectra of warm supergiants, *Astrophys. J. Lett.* 365 (1990) L23–L26. doi:10.1086/185879.
- [73] E. Peeters, A. G. G. M. Tielens, P. R. Roelfsema, P. Cox, PAHs in compact HII regions, in: P. Cox, M. Kessler (Eds.), *The Universe as Seen by ISO*, Vol. 427 of ESA Special Publication, 1999, p. 739.
- [74] R. J. Laureijs, D. Watson, L. Metcalfe, B. McBreen, B. O'Halloran, J. Clavel, K. Leech, P. Gallais, P. Barr, M. Delaney, L. Hanlon, F. Quilligan, ISO observations of a sample of 60  $\mu\text{m}$  peaker galaxies, *Astron. Astrophys.* 359 (3) (2000) 900–906.

- [75] N. L. J. Cox, P. Pilleri, O. BernÅ©, J. Cernicharo, C. Joblin, Polycyclic aromatic hydrocarbons and molecular hydrogen in oxygen-rich planetary nebulae: the case of ngc 6720, *Monthly Notices of the Royal Astronomical Society: Letters* 456 (1) (2016) L89–L93. doi:10.1093/mnrasl/slv184.  
URL <http://dx.doi.org/10.1093/mnrasl/slv184>
- [76] D. M. Hudgins, S. A. Sandford, Infrared spectroscopy of matrix isolated polycyclic aromatic hydrocarbons. 2. pahs containing five or more rings, *The Journal of Physical Chemistry A* 102 (2) (1998) 344–352. arXiv:<https://doi.org/10.1021/jp983482y>, doi:10.1021/jp983482y.  
URL <https://doi.org/10.1021/jp983482y>

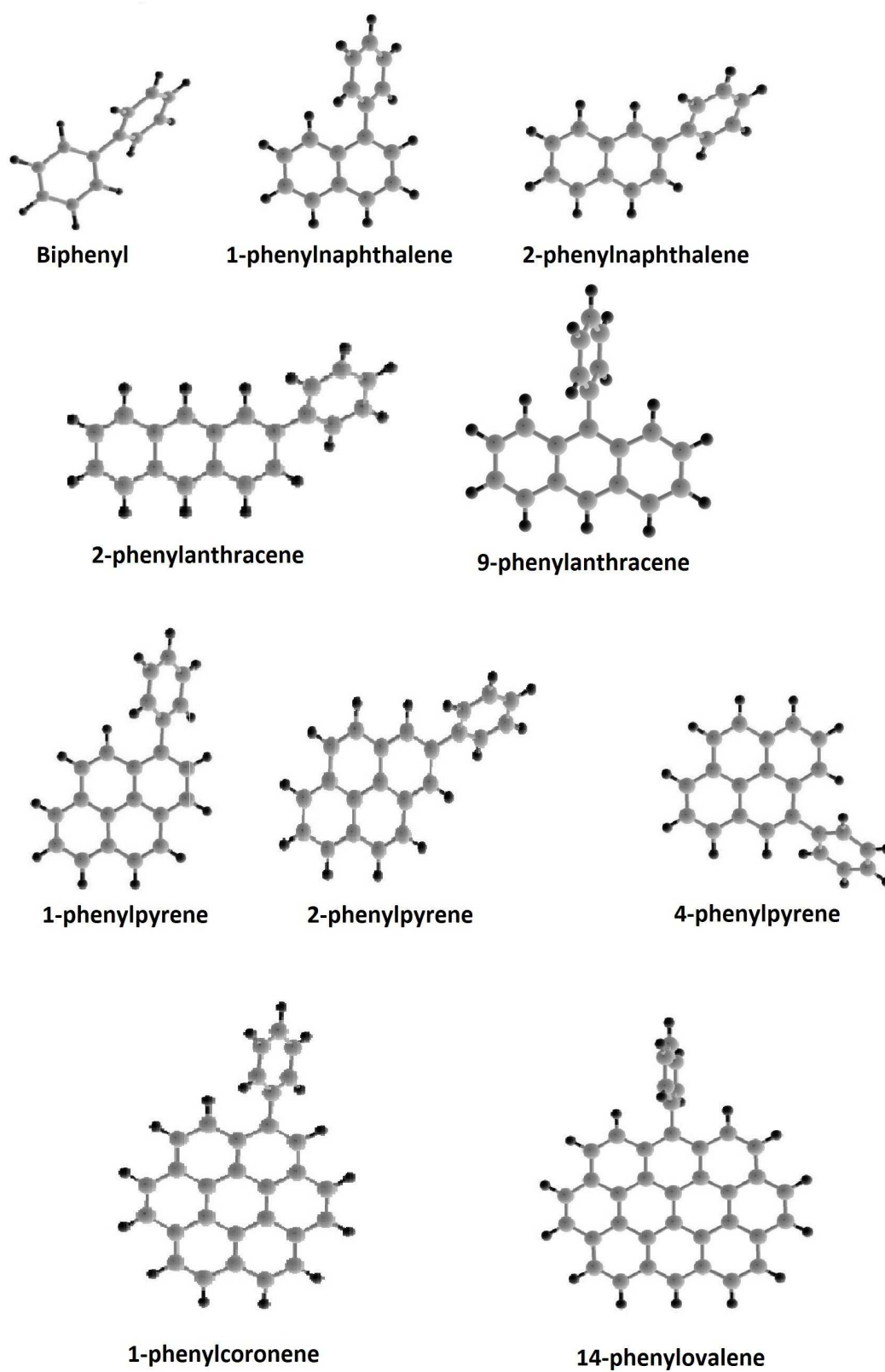


Figure 1: Molecular structures of the studied phenyl-PAHs.

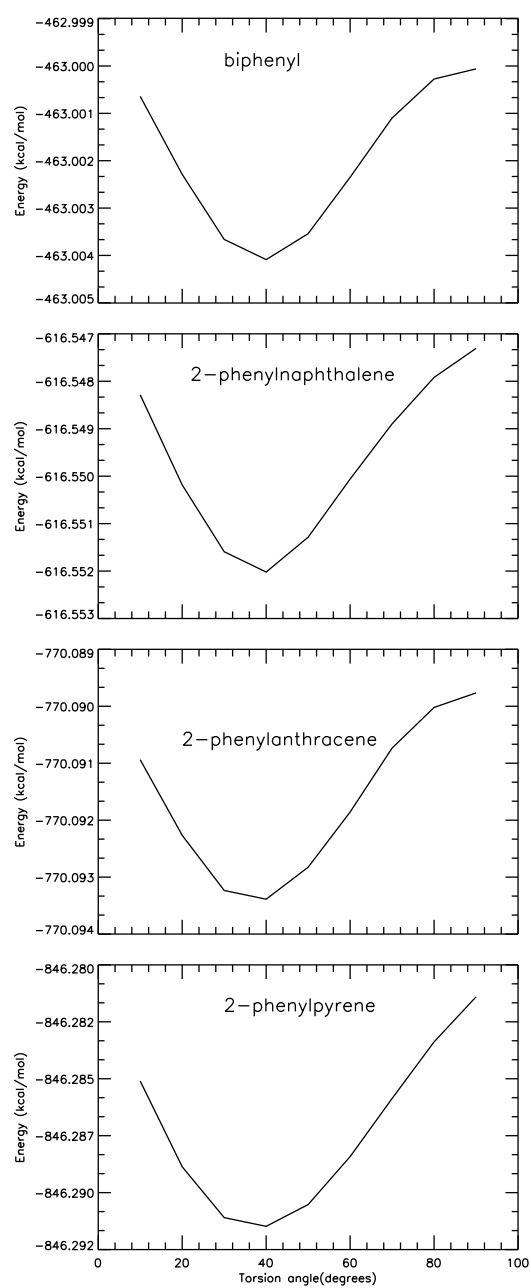


Figure 2a: Variation of optimization energy with torsion angle of the phenyl group substituted in symmetric H placement.

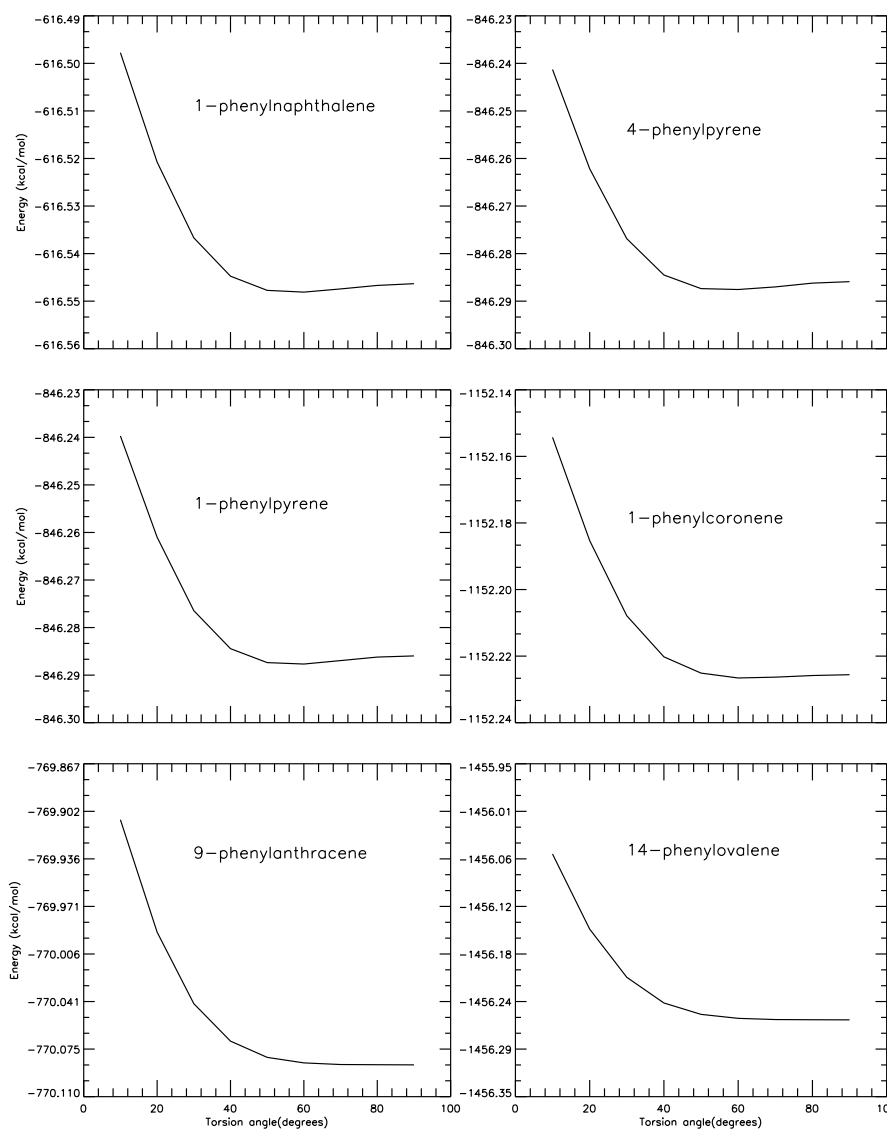


Figure 2b: Variation of optimization energy with torsion angle of the phenyl group substituted in asymmetric H placement and at solo position.

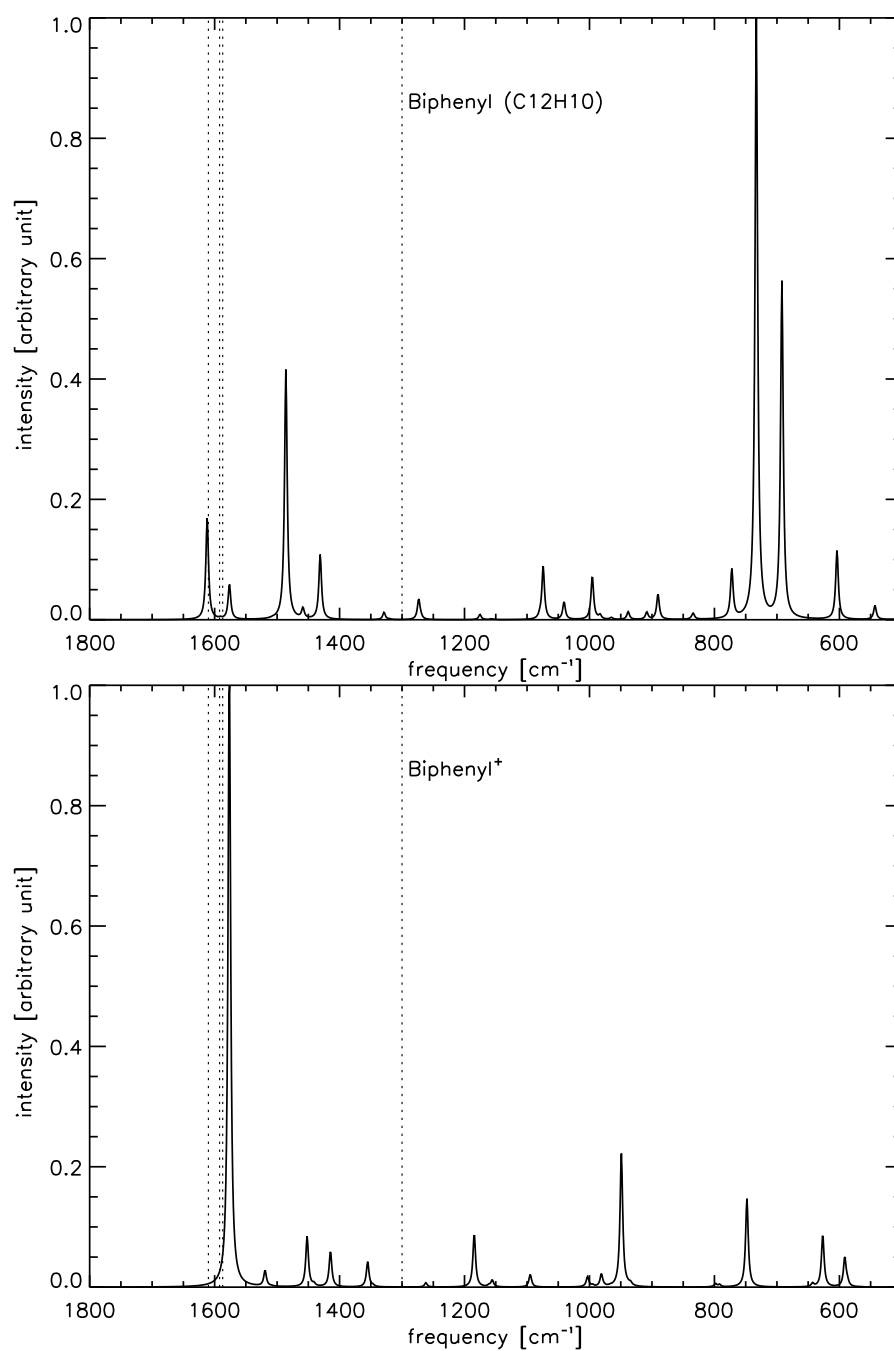


Figure 3: Computed infrared spectra of Biphenyl neutral and cation.

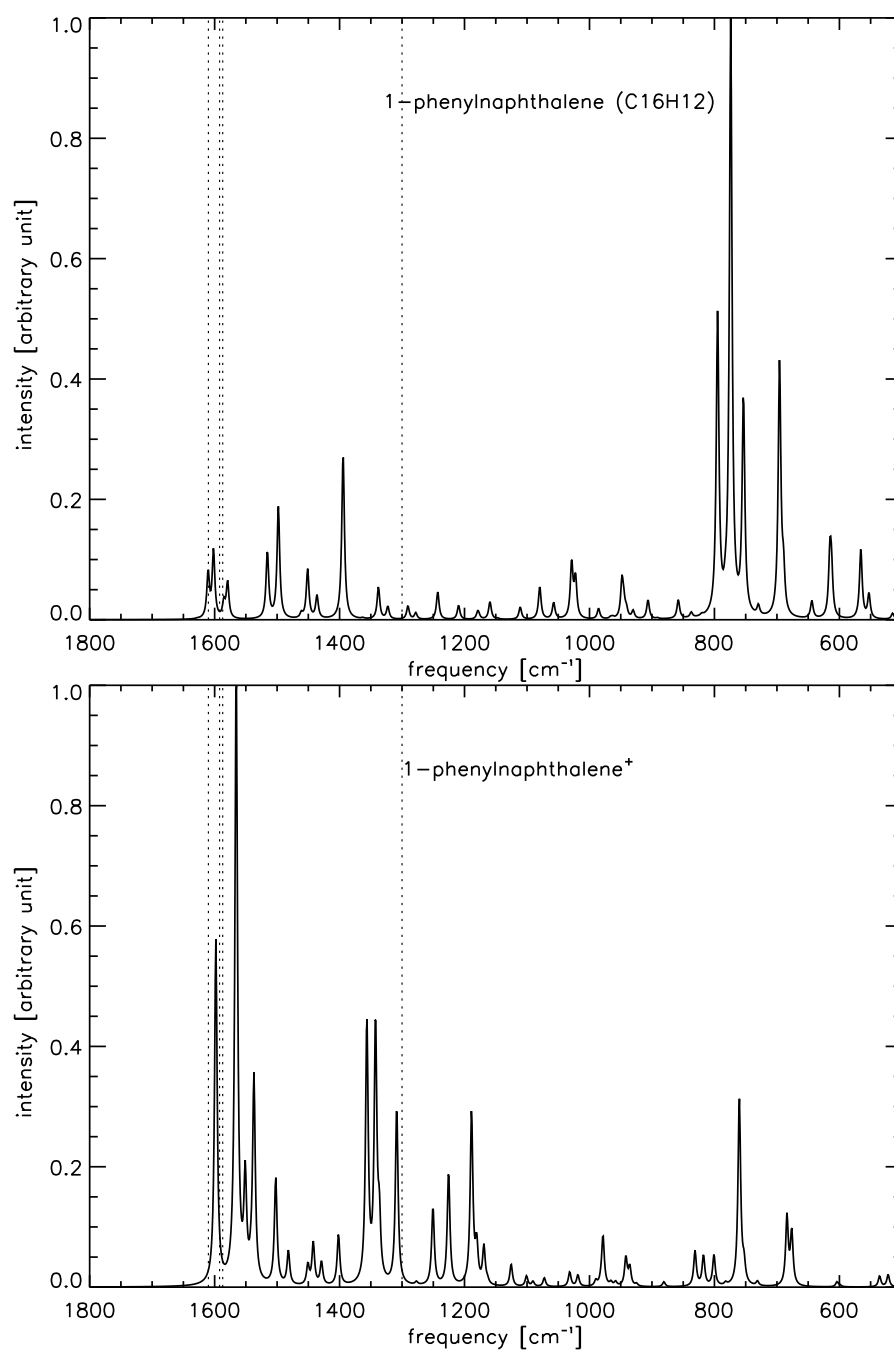


Figure 4: Computed infrared spectra of 1-phenylnaphthalene neutral and cation.

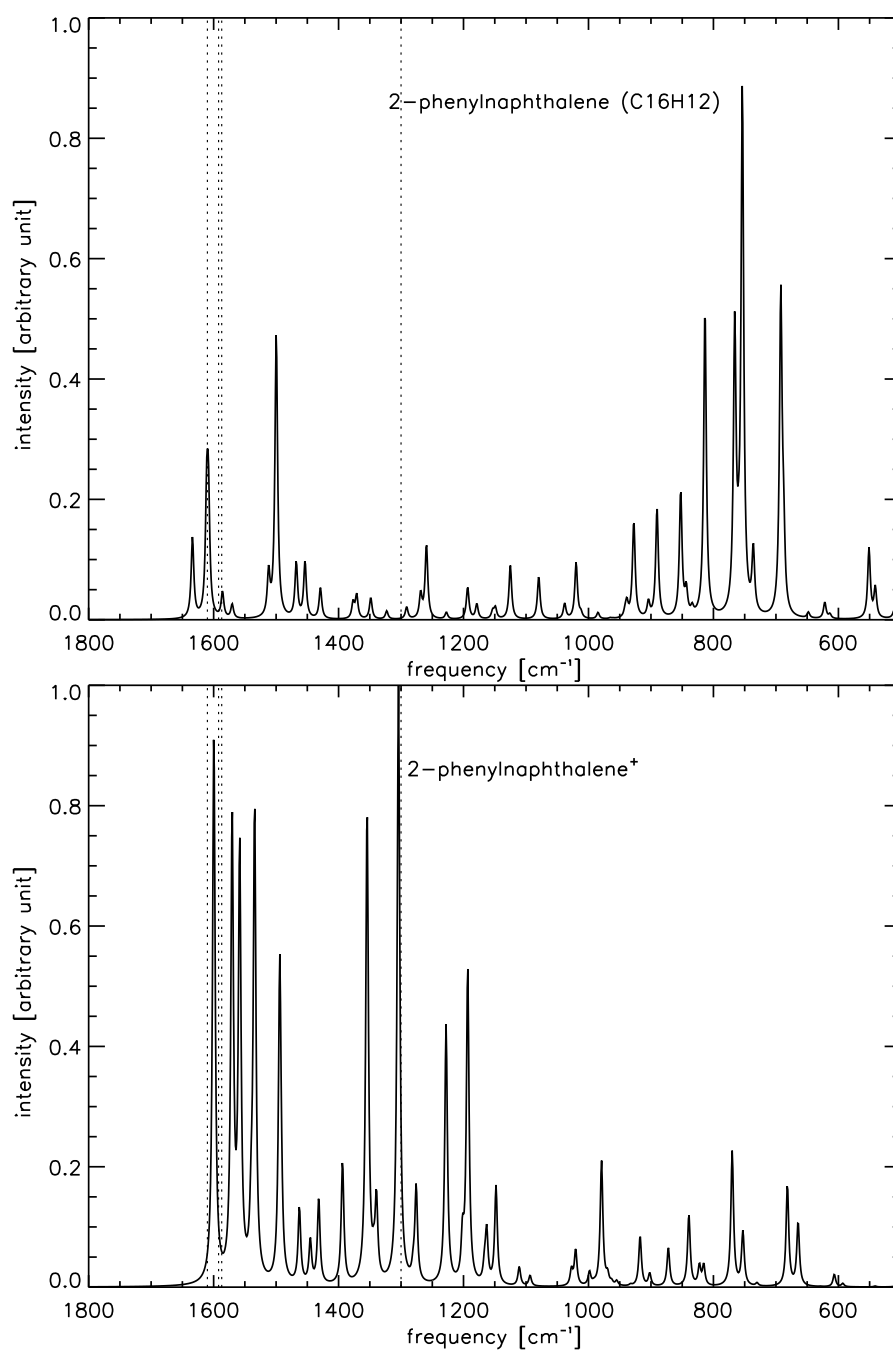


Figure 5: Computed infrared spectra of 2-phenylnaphthalene neutral and cation.

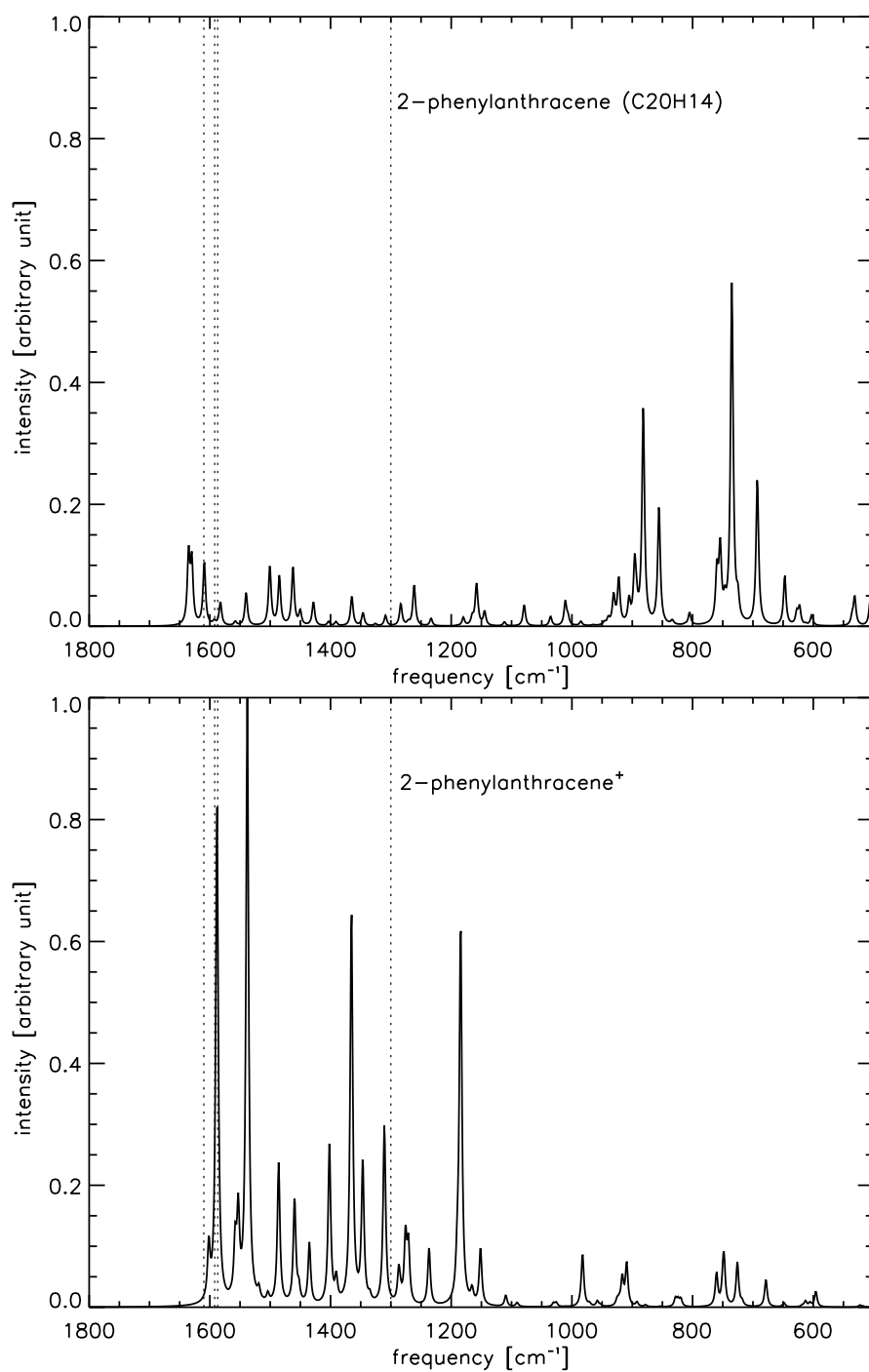


Figure 6: Computed infrared spectra of 2-phenylanthracene neutral and cation.

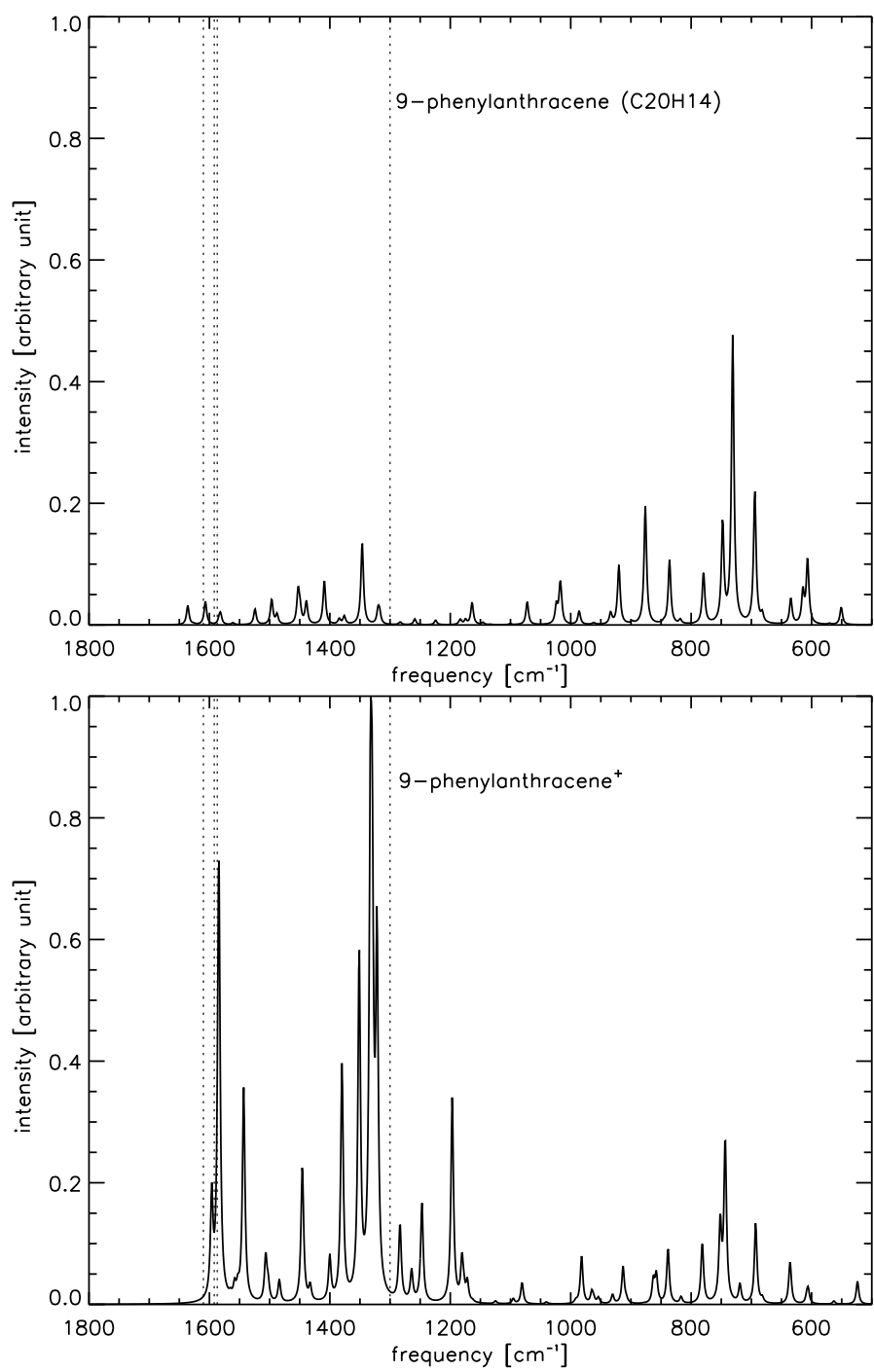


Figure 7: Computed infrared spectra of 9-phenylanthracene neutral and cation.

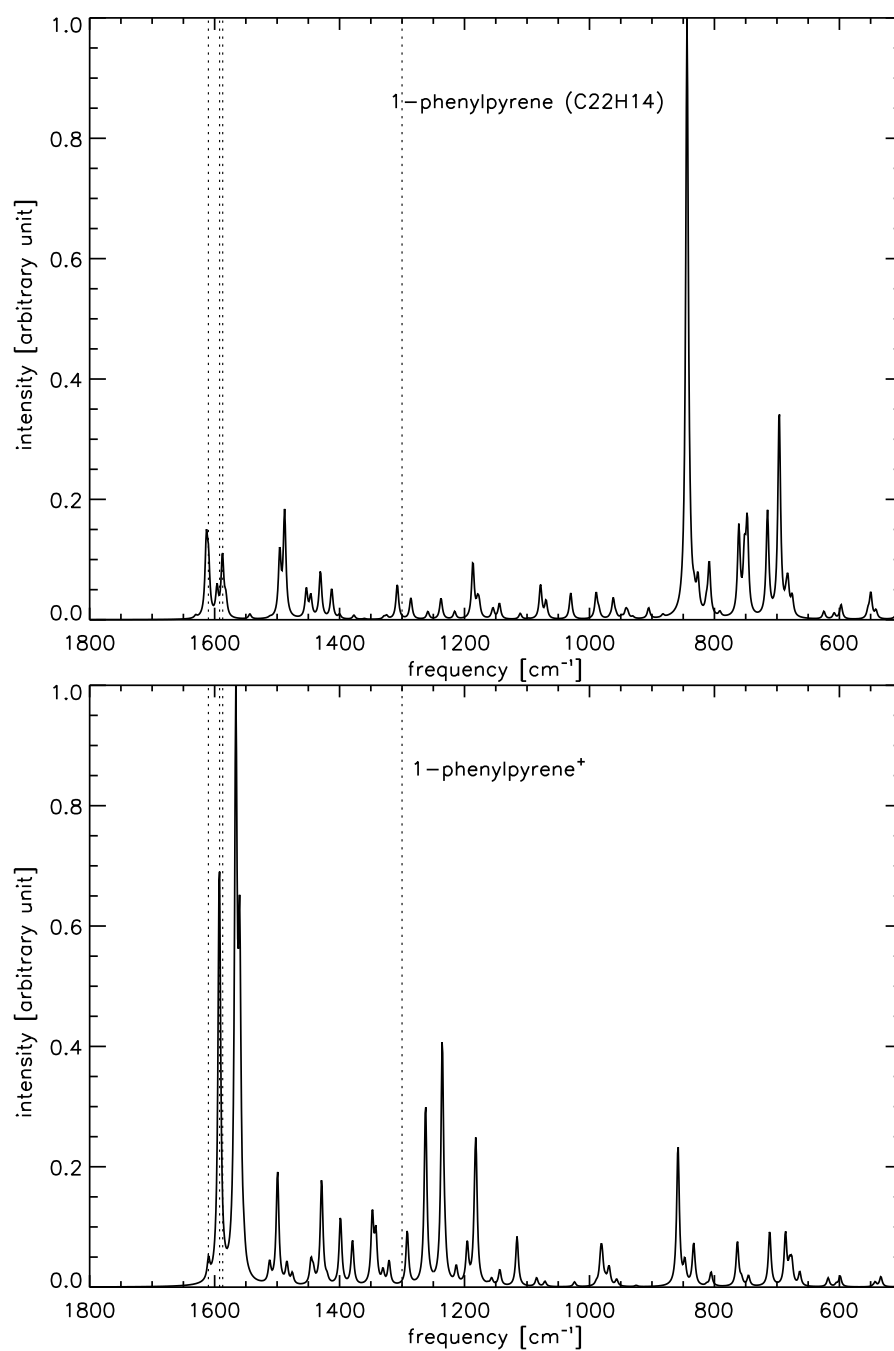


Figure 8: Computed infrared spectra of 1-phenylpyrene neutral and cation.

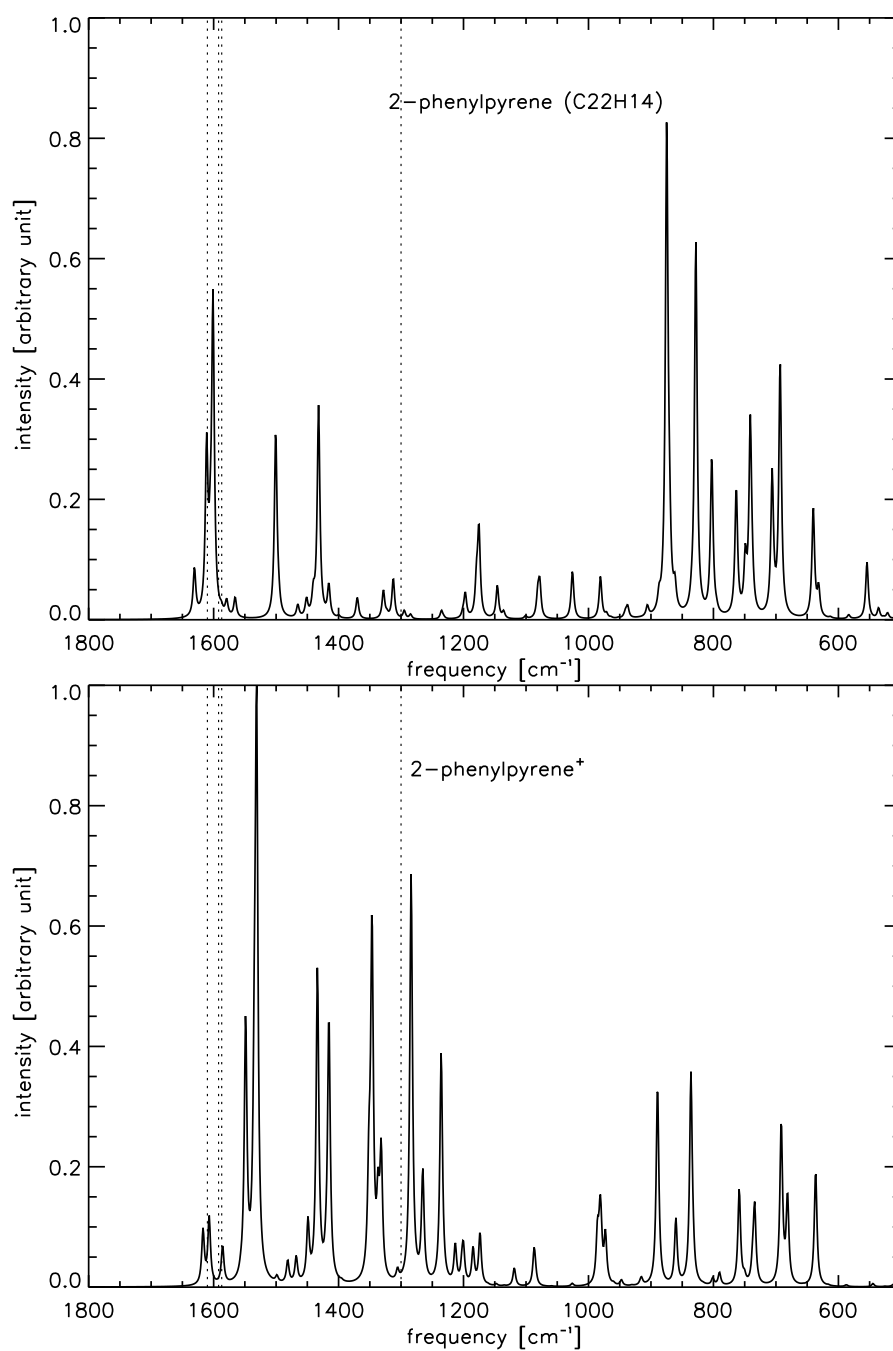


Figure 9: Computed infrared spectra of 2-phenylpyrene neutral and cation.

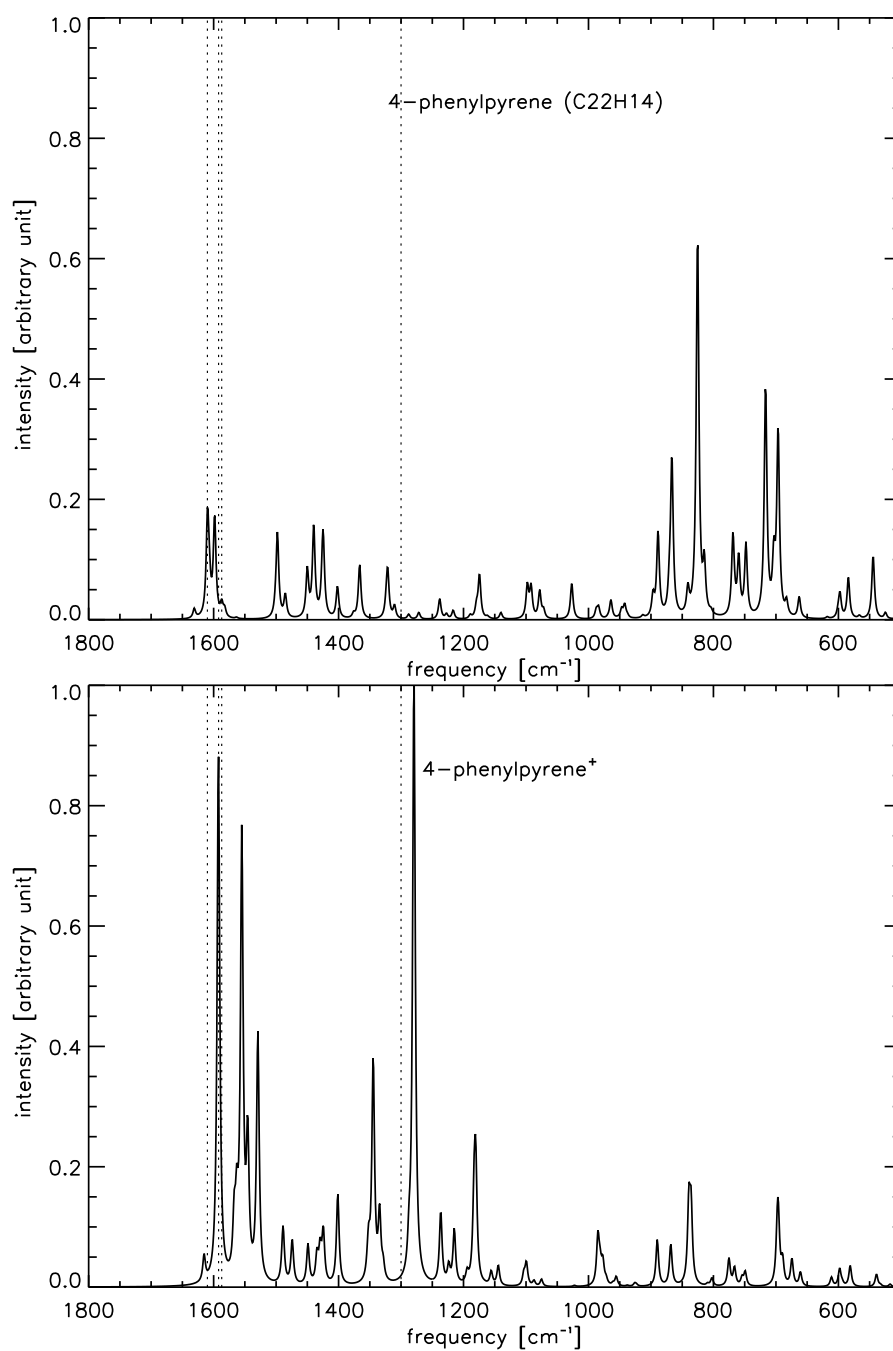


Figure 10: Computed infrared spectra of 4-phenylpyrene neutral and cation.

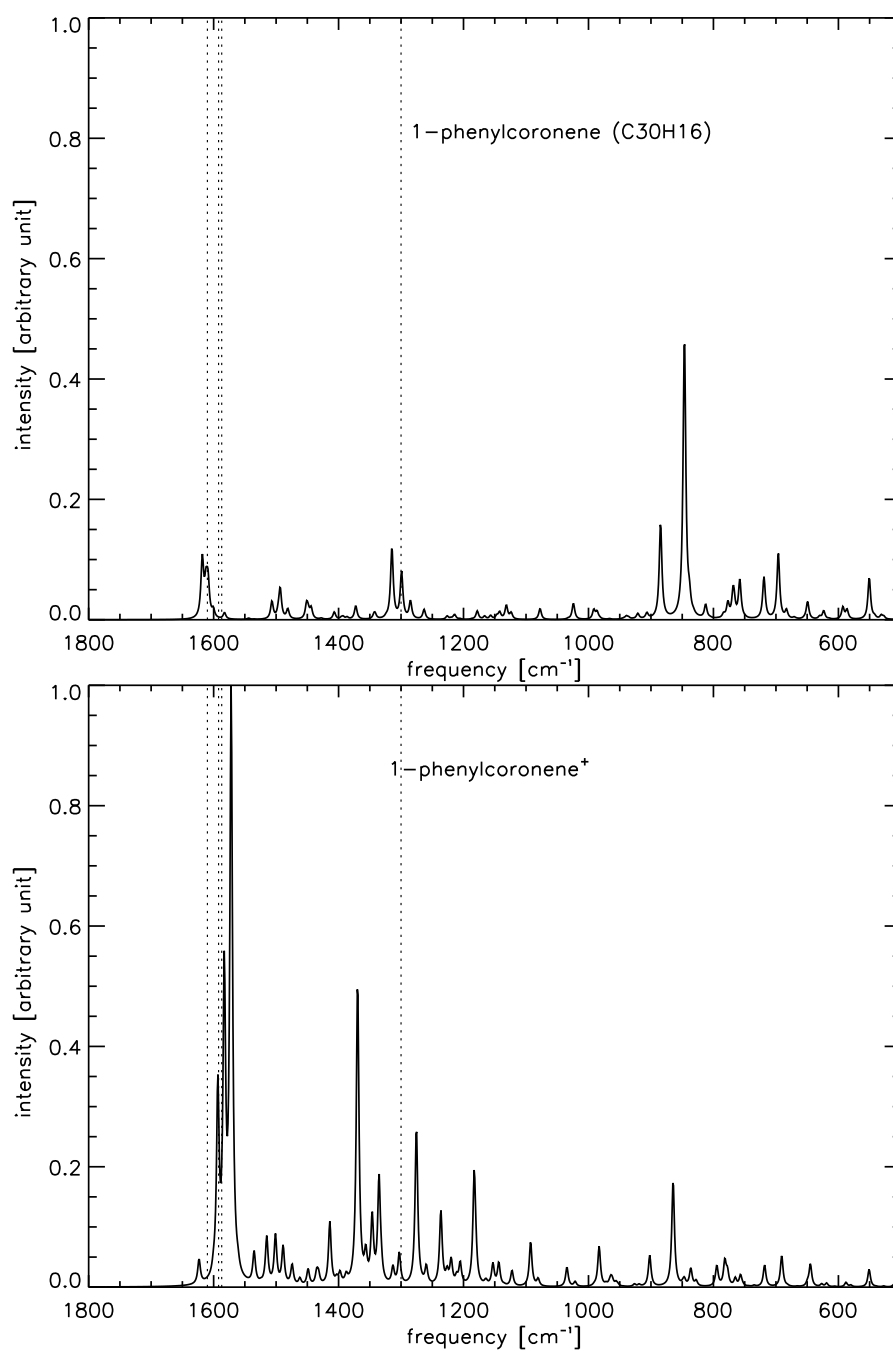


Figure 11: Computed infrared spectra of 1-phenylcoronene neutral and cation.

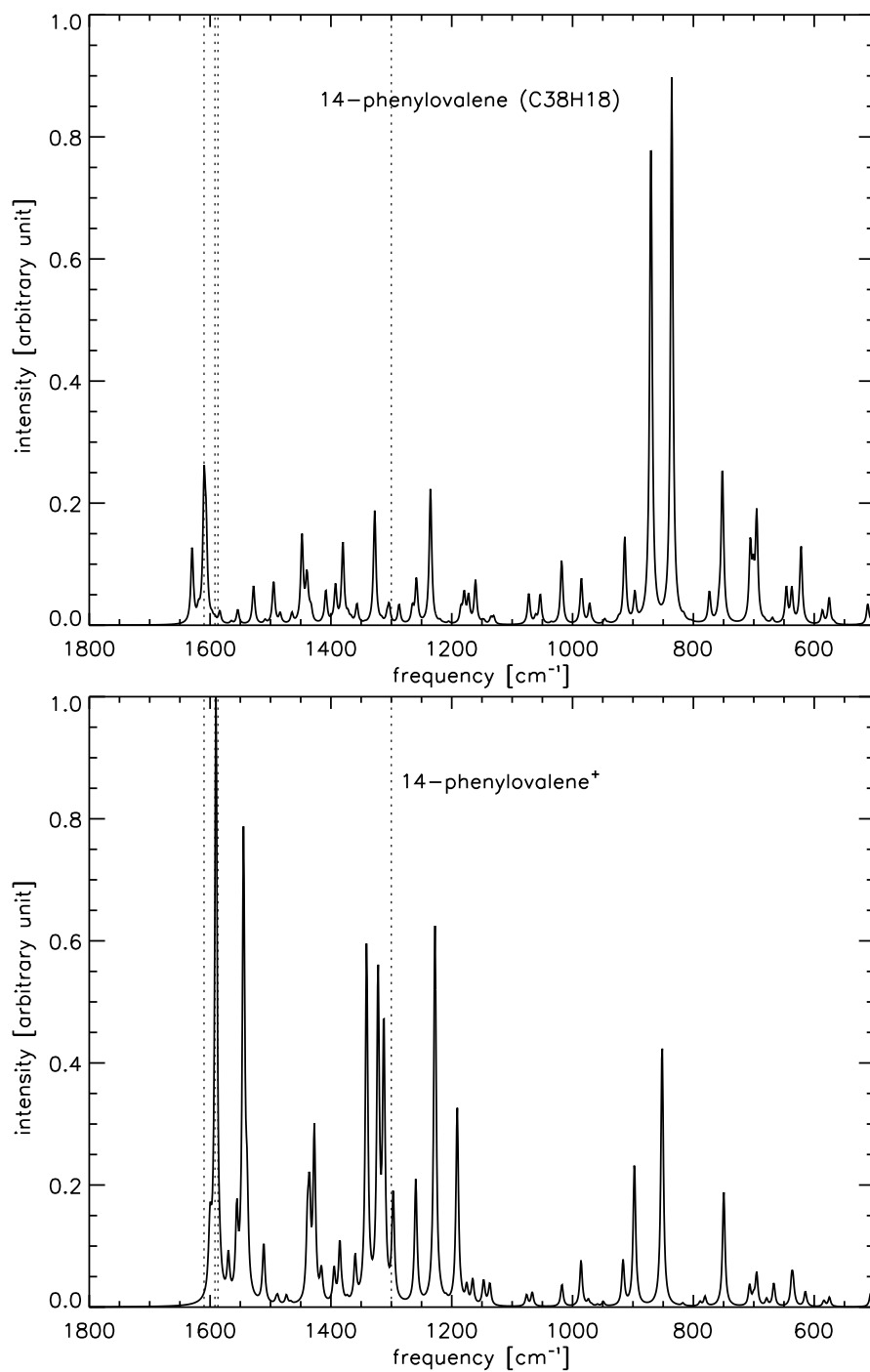


Figure 12: Computed infrared spectra of 14-phenylvalene neutral and cation.

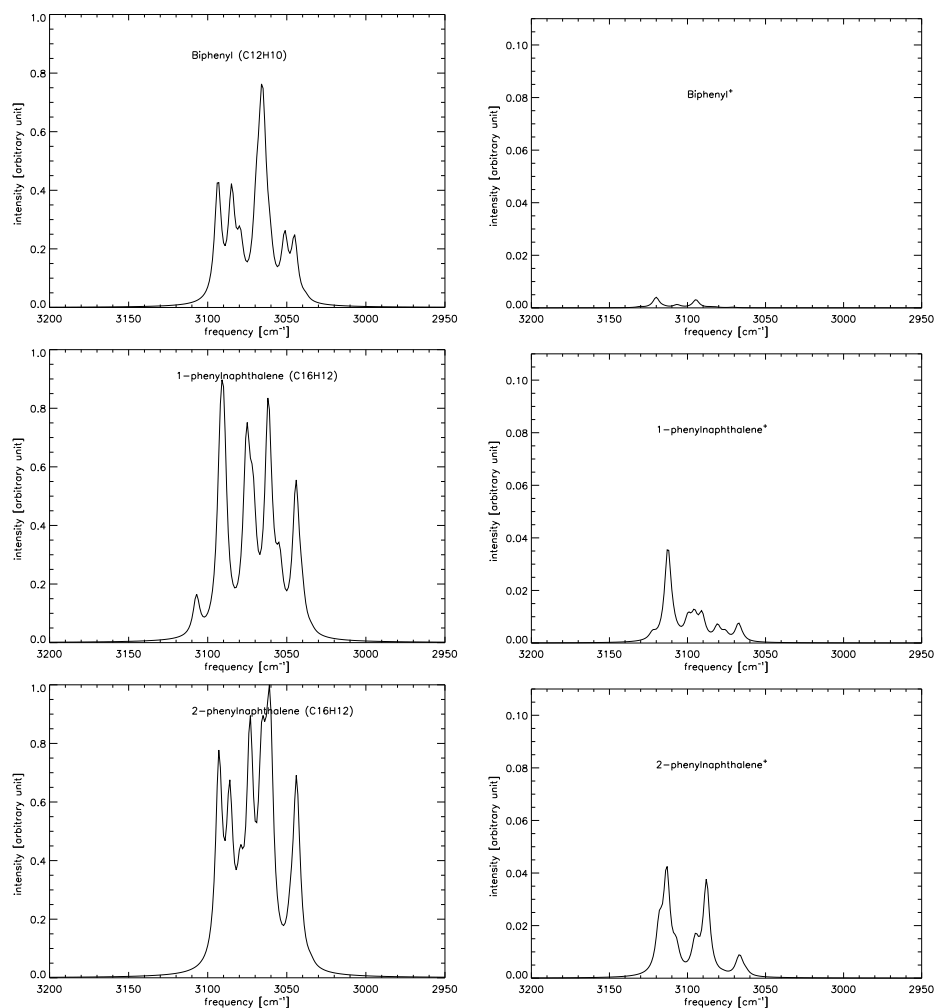


Figure 13a: The C-H stretch spectral region of infrared spectra in neutrals and cations of biphenyl and phenylnaphthalenes

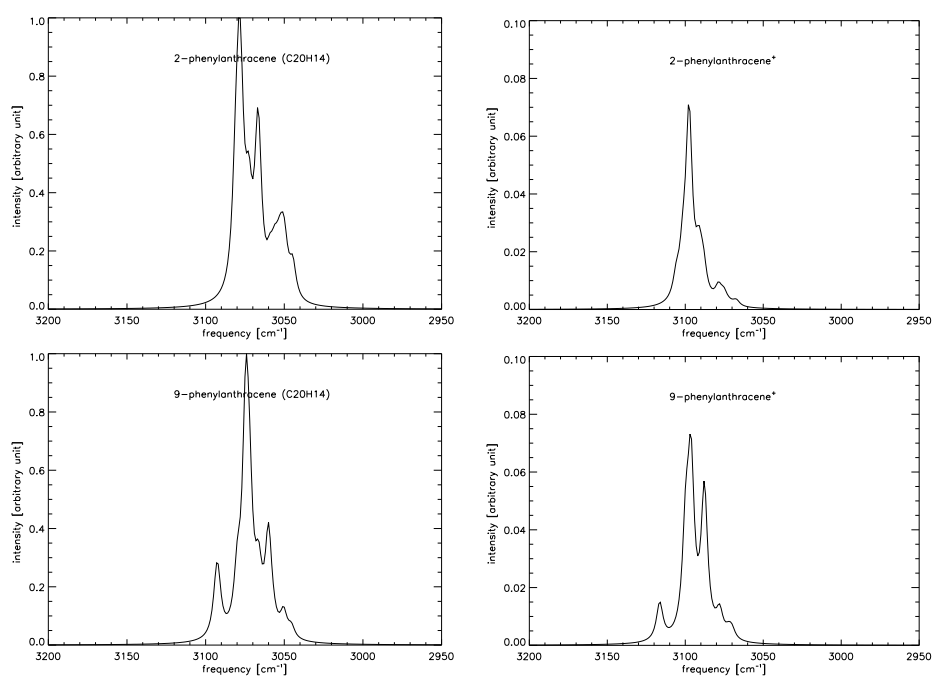


Figure 13b: The C-H stretch spectral region of infrared spectra in neutrals and cations of phenylanthracenes.

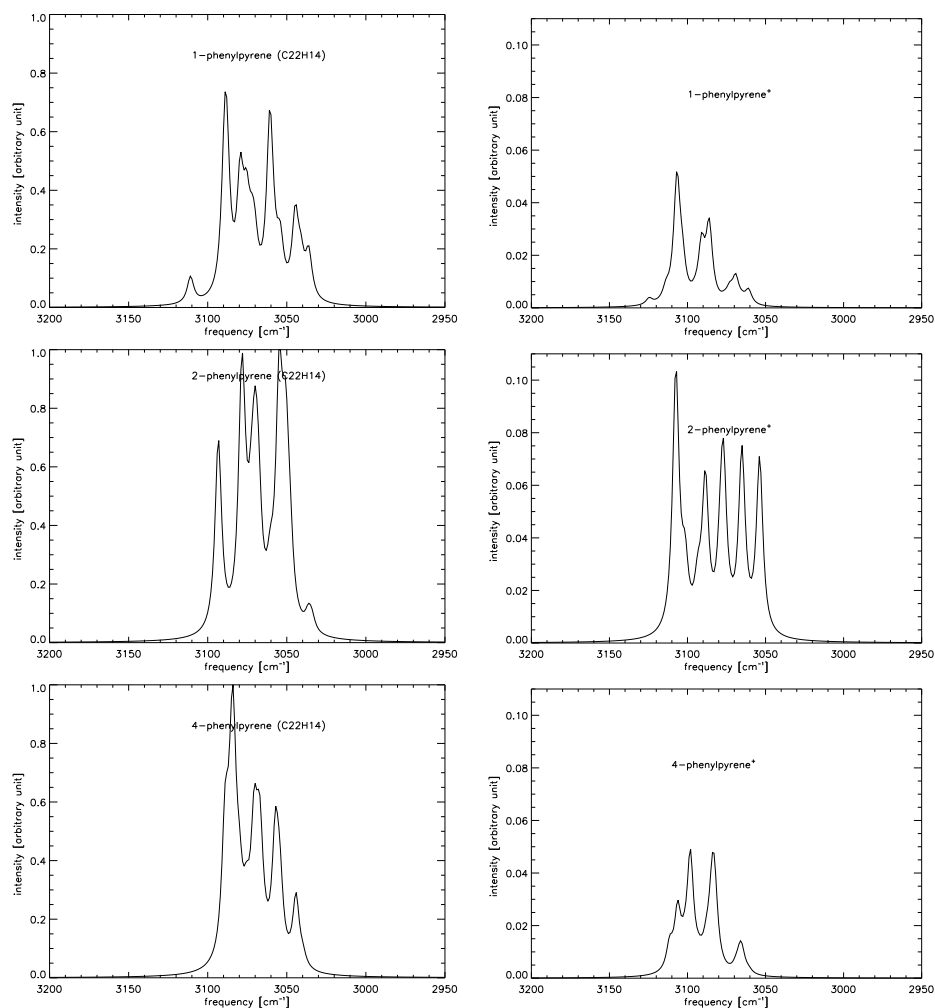


Figure 13c: The C-H stretch spectral region of infrared spectra in neutrals and cations of phenylpyrenes.

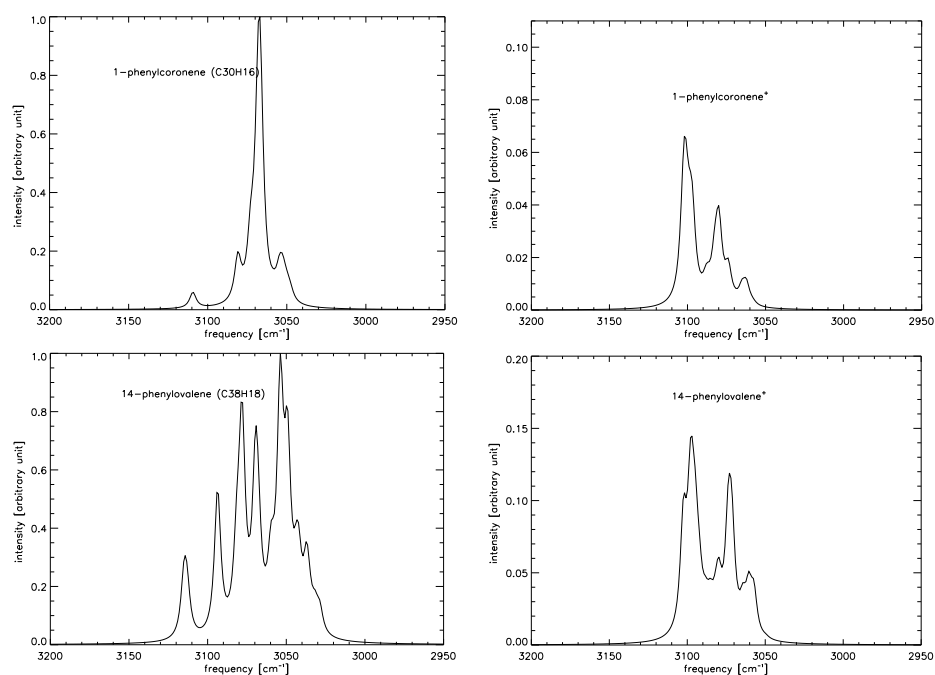


Figure 13d: The C-H stretch spectral region of infrared spectra in neutrals and cations of phenylcoronene and phenylvalene.

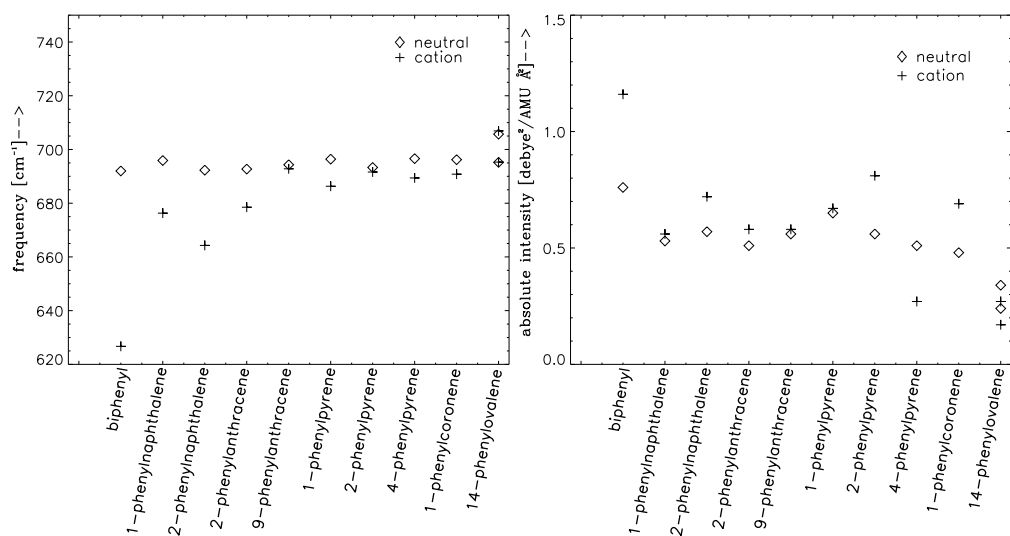


Figure 14: The frequency and the absolute intensity of the phenyl C-H wag mode in 710 - 690  $\text{cm}^{-1}$  region is plotted for both neutral and cation.

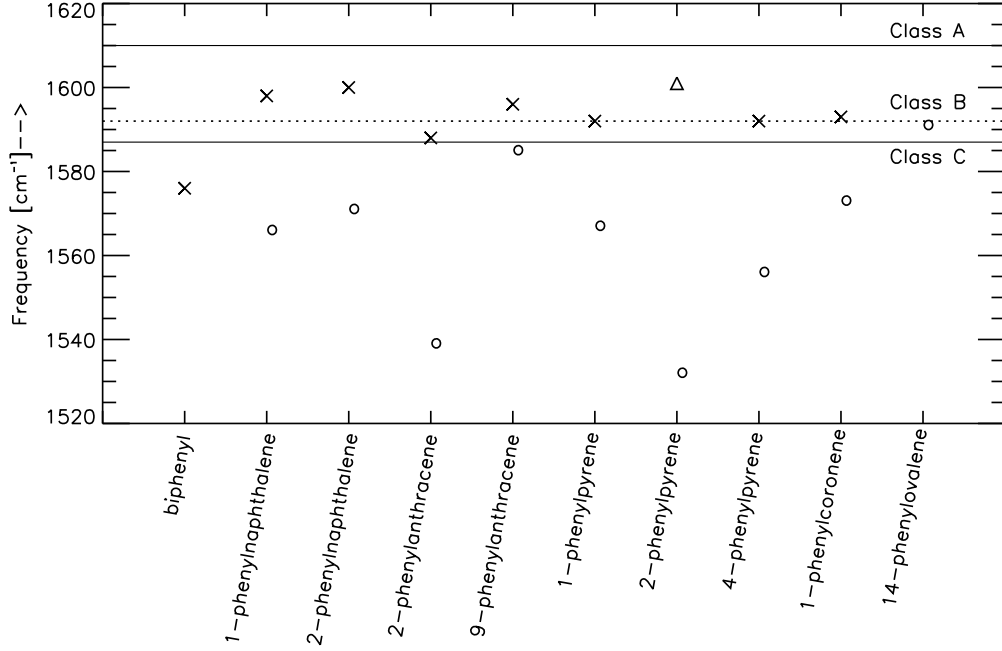


Figure 15: The position of modes near  $6.2 \mu\text{m}$  AIB in phenyl-PAH cations; ‘ $\times$ ’ - C-C stretch in phenyl unit and ‘o’ - C-C stretch in PAH moiety; ‘ $\Delta$ ’ - phenyl C-C stretch in neutral 2-phenylpyrene.

Table 1: Optimized geometry-phenyl group torsion angle and energies

| Phenyl-PAHs         | torsion angle (degree) |        | optimization energy (Kcal/mol) |               | Energy change<br>$\Delta E$ |
|---------------------|------------------------|--------|--------------------------------|---------------|-----------------------------|
|                     | neutral                | cation | neutral                        | cation        |                             |
| Biphenyl            | 39.09                  | 19.69  | -463.0040821                   | -462.7266937  | -0.2774                     |
| 1-phenylnaphthalene | 57.48                  | 40.04  | -616.5482200                   | -616.2894685  | -0.2588                     |
| 2-phenylnaphthalene | 38.45                  | 26.47  | -616.5521073                   | -616.2921034  | -0.2600                     |
| 2-phenylanthracene  | 37.3                   | 29.6   | -770.0938302                   | -769.8543519  | -0.2395                     |
| 9-phenylanthracene  | 80.6                   | 58.7   | -770.0865564                   | -769.8478848  | -0.2387                     |
| 1-phenylpyrene      | 54.93                  | 46.65  | -846.2877170                   | -846.0481901  | -0.2395                     |
| 2-phenylpyrene      | 38.12                  | 36.44  | -846.2910842                   | -846.0439777  | -0.2471                     |
| 4-phenylpyrene      | 53.47                  | 46.94  | -846.2876183                   | -846.0457597  | -0.2419                     |
| 1-phenylcoronene    | 59.05                  | 48.08  | -1152.2268317                  | -1151.9875017 | -0.2381                     |
| 14-phenylvalene     | 90.00                  | 90.10  | -1458.1499689                  | -1457.9303203 | -0.2196                     |

Table 2: Comparison of corresponding C-H out-of-plane vibrational frequencies between neutral and ionized Phenyl-PAHs

| Phenyl-PAHs         | frequency ( $\text{cm}^{-1}$ ) |                |             | absolute intensity<br>(Debye <sup>2</sup> /AMU $\text{\AA}^2$ ) |        | intensity<br>$\Delta_{fractional-difference}^*$ |
|---------------------|--------------------------------|----------------|-------------|---|--------|---|
|                     | $\nu_{neutral}$                | $\nu_{cation}$ | $\Delta\nu$ | neutral   | cation |   |
| Biphenyl            | 692.0 <sup>a</sup>             | 626.7          | 65.3        | 0.76  | 1.11   | -0.46   |
|                     | 732.9 <sup>a</sup>             | 748.1          | -15.2       | 1.07  | 1.93   | -0.51   |
|                     | 733.2 <sup>a</sup>             | —              | —           | 0.55  | —      | —   |
| 1-phenylnaphthalene | 695.9 <sup>a</sup>             | 676.3          | 19.6        | 0.53  | 0.56   | -0.06   |
|                     | 753.6 <sup>a</sup>             | 752.7          | 0.9         | 0.46  | 0.19   | 0.59  |
|                     | 774.0                          | 760.2          | 13.8        | 1.25  | 1.96   | -0.57   |
| 2-phenylnaphthalene | 794.9                          | 800.7          | -5.8        | 0.63  | 0.32   | 0.49  |
|                     | 692.3 <sup>a</sup>             | 664.3          | 28.0        | 0.57  | 0.72   | -0.26   |
|                     | 753.7                          | 770.0          | -16.3       | 0.92  | 1.53   | -0.66   |
| 2-phenylanthracene  | 765.9                          | 752.6          | 13.3        | 0.50  | 0.31   | 0.38  |
|                     | 813.5                          | 872.2          | -58.7       | 0.55  | 0.44   | 0.20  |
|                     | 692.7 <sup>a</sup>             | 678.5          | 14.2        | 0.51  | 0.58   | -0.14   |
| 9-phenylanthracene  | 735.1                          | 747.9          | -12.7       | 1.05  | 0.79   | 0.25  |
|                     | 881.8                          | 909.2          | -27.4       | 0.75  | 0.90   | -0.20   |
|                     | 694.3 <sup>a</sup>             | 692.8          | 1.5         | 0.56  | 0.58   | -0.04   |
| 1-phenylpyrene      | 731.0                          | 743.5          | -12.5       | 1.21  | 1.16   | 0.04  |
|                     | 747.7 <sup>a</sup>             | 751.7          | -4.0        | 0.42  | 0.56   | -0.33   |
|                     | 876.1                          | 913.1          | -37.0       | 0.50  | 0.27   | 0.46  |
| 2-phenylpyrene      | 696.4 <sup>a</sup>             | 686.3          | 10.1        | 0.65  | 0.67   | -0.03   |
|                     | 747.5                          | 745.5          | 2.0         | 0.28  | 0.13   | 0.53  |
|                     | 752.0                          | 756.8          | -4.8        | 0.18  | 0.08   | 0.55  |
| 4-phenylpyrene      | 761.0 <sup>a</sup>             | 763.3          | -2.3        | 0.28  | 0.57   | -1.04   |
|                     | 843.9                          | 858.4          | -14.5       | 1.89  | 1.81   | 0.04  |
|                     | 693.3 <sup>a</sup>             | 691.6          | 1.7         | 0.56  | 0.81   | -0.45   |
| 1-phenylcoronene    | 741.0                          | 734.1          | 6.9         | 0.42  | 0.38   | 0.10  |
|                     | 763.5                          | 758.7          | 4.8         | 0.29  | 0.48   | -0.66   |
|                     | 828.2                          | 836.1          | -7.9        | 0.84  | 1.05   | -0.25   |
| 14-phenylovalene    | 874.8                          | 889.5          | -14.7       | 1.08  | 1.00   | 0.07  |
|                     | 696.6 <sup>a</sup>             | 689.4          | 7.2         | 0.50  | 0.28   | 0.44  |
|                     | 748.0                          | 749.2          | -1.2        | 0.20  | 0.16   | 0.20  |
| 1-phenylpyrene      | 768.8 <sup>a</sup>             | 766.3          | 2.5         | 0.22  | 0.21   | 0.05  |
|                     | 825.5                          | 839.3          | -13.8       | 1.05  | 0.90   | 0.14  |
|                     | 866.6                          | 889.9          | -23.3       | 0.43  | 0.54   | -0.26   |
| 1-phenylcoronene    | 696.2 <sup>a</sup>             | 690.8          | 5.4         | 0.48  | 0.69   | -0.44   |
|                     | 757.8 <sup>a</sup>             | 765.0          | -7.2        | 0.28  | 0.17   | 0.39  |
|                     | 846.3                          | 864.6          | -18.3       | 1.47  | 2.38   | -0.62   |
| 14-phenylovalene    | 846.8                          | —              | —           | 0.62  | —      | —   |
|                     | 884.6                          | 902.0          | -17.4       | 0.70  | 0.70   | 0.00  |
|                     | 695.2 <sup>a</sup>             | 695.3          | -0.1        | 0.33  | 0.25   | 0.24  |
| 14-phenylovalene    | 705.7 <sup>a</sup>             | 706.9          | -1.2        | 0.24  | 0.17   | 0.29  |
|                     | 752.0 <sup>a</sup>             | 749.7          | 2.3         | 0.50  | 0.95   | -0.90   |
|                     | 835.8                          | 851.8          | -16.0       | 1.75  | 2.20   | -0.26   |
| 14-phenylovalene    | 870.3                          | 897.6          | -27.3       | 1.57  | 1.19   | 0.24  |

\*the fractional difference of intensity is defined as  $\Delta = (\text{neutral-cation})/\text{neutral}$ . <sup>a</sup>Phenyl C-H wag mode.

Table 3: Comparison of out-of-plane vibrations of phenyl-PAHs to the C-H out-of-plane vibrations in the corresponding plain PAHs. The unit of the frequencies given in the table is in  $\text{cm}^{-1}$  and the corresponding relative intensities are given in parenthesis. In column A the out-of-plane frequencies and relative intensities of phenyl-PAHs are given and in column B the out-of-plane frequencies and relative intensities of corresponding plain PAHs are given.

| Phenyl-PAHs         | Solo modes frequencies |                          | Duo modes frequencies |                          | trio modes frequencies |                          | Quarto modes frequencies |                          |
|---------------------|------------------------|--------------------------|-----------------------|--------------------------|------------------------|--------------------------|--------------------------|--------------------------|
|                     | A                      | B                        | A                     | B                        | A                      | B                        | A                        | B                        |
| 1-phenylnaphthalene | —                      | —                        | —                     | —                        | —                      | —                        | 774.0(1.00)              | —                        |
|                     | —                      | —                        | —                     | —                        | —                      | —                        | 794.9(0.50)              | 788.2(1.00) <sup>a</sup> |
| 2-phenylnaphthalene | —                      | —                        | —                     | —                        | —                      | —                        | 753.7(1.00)              | —                        |
|                     | —                      | —                        | —                     | —                        | —                      | —                        | 765.9(0.54)              | —                        |
|                     | —                      | —                        | —                     | —                        | —                      | —                        | 813.5(0.60)              | 788.2(1.00) <sup>a</sup> |
| 2-phenylanthracene  | 881.8(0.65)            | 878.3(0.77) <sup>a</sup> | —                     | —                        | —                      | —                        | 735.1(0.91)              | 729.6(1.00) <sup>a</sup> |
| 9-phenylanthracene  | 876.1(0.39)            | 878.3(0.77) <sup>a</sup> | —                     | —                        | —                      | —                        | 731.0(0.95)              | 729.6(1.00) <sup>a</sup> |
| 1-phenylpyrene      | —                      | —                        | 843.9(1.00)           | 842.8(1.00) <sup>a</sup> | 747.5(0.15)            | —                        | —                        | —                        |
|                     | —                      | —                        | —                     | —                        | 752.0(0.10)            | 743.9(0.17) <sup>a</sup> | —                        | —                        |
| 2-phenylpyrene      | —                      | —                        | 828.2(0.78)           | 842.8(1.00) <sup>a</sup> | 741.0(0.39)            | 743.9(0.17) <sup>a</sup> | —                        | —                        |
|                     | —                      | —                        | 874.8(1.00)           | —                        | 763.5(0.27)            | —                        | —                        | —                        |
| 4-phenylpyrene      | —                      | —                        | 825.5(0.90)           | 842.8(1.00) <sup>a</sup> | 748.0(0.17)            | 743.9(0.17) <sup>a</sup> | —                        | —                        |
|                     | —                      | —                        | 866.6(0.37)           | —                        | —                      | —                        | —                        | —                        |
| 1-phenylcoronene    | —                      | —                        | 846.5(1.00)           | 857.0(1.00) <sup>a</sup> | —                      | —                        | —                        | —                        |
|                     | —                      | —                        | 884.6(0.36)           | —                        | —                      | —                        | —                        | —                        |
| 14-phenylovalene    | 870.3(0.90)            | 901.9(0.99) <sup>b</sup> | 835.8(1.00)           | 847.4(0.71) <sup>b</sup> | —                      | —                        | —                        | —                        |

<sup>a</sup>Data taken from Hudgins1998a [59] and Hudgins1998b [76] for the observed Infrared frequencies in the corresponding plain PAHs. <sup>b</sup> Theoretical data taken from Pathak 2006 [46].